EXOPLANET TRANSIT STUDIES OF WASP-12b

Project By
Asmita E. Bhandare
BSc Physics -Final Year
Fergusson College,
Pune, India.

In partial fulfillment for the award of the degree

of

Bachelors in Physics

Fergusson College

University of Pune, Pune - 411007

March 2012

Deccan Education Society's

FERGUSSON COLLEGE, PUNE

DEPARTMENT OF PHYSICS

CERTIFICATE

This is to certify that Miss Bhandare Asmita Eknath Roll No. 647 Examination Seat No._____ of the T.Y.B.Sc. Physics class of this department has successfully completed the project entitled "Exoplanet Transit Studies of WASP-12b" as partial fulfillment of the B.Sc (Physics) degree of the University of Pune during the academic year 2011-12.

Internal Guide

Dr. R.V. Dabhade

External Guide

Dr. Firoza Sutaria

Dr. D. D. Choughule

Head, Dept. of Physics

Examiner-I

Examiner-II

CERTIFICATE

दूरभाष Ph : 91-80-25530672-76
फैक्स Fax : 91-80-25534043
तार Grams : ASTRON

भारतीय ताराभौतिकी संस्थान
INDIAN INSTITUTE OF ASTROPHYSICS
कोरमंगला / KORAMANGALA
बेंगलूर / BANGALORE - 560 034.

IIA/Per. Div/BGS/2011
June 13, 2010

Ms. Asmita Eknath Bhandare,
Fergusson College,
Pune.

Dear Ms.Asmita Eknath Bhandare,

Kindly refer to your letter dated and to inform you that, permission has been granted to visit IIA under Visiting Students Internship Programme. You will be working under the guidance of Dr.Firoza K Sutaria, Reader of this Institute. Your visit to IIA will be for a period of TWO months starting from June 15, 2011. During this period you will be provided with rent free shared accommodation and permitted to use Library (reference only), computing and canteen facilities at the subsidized rates. Kindly contact the undersigned, in person, to complete administrative formalities.

Yours faithfully,

A.Narasimharaju
Personnel ~~officer~~
for Director

CC to Dr. Firoza K. Sutaria and all concerned

CERTIFICATE

INDIAN INSTITUTE OF ASTROPHYSICS

(Ministry of Science and Technology, Govt. of India)

KORAMANGALA, BANGALORE

SUMMER PROGRAMMES – 2011

This is to certify that Ms. Asmita Bhandare participated in the Summer Internship Programme 2011 held during the period of 15 June – 15 August 2011 at this Institute. Her project was titled "Exoplanet Transit Studies of WASP-12b" and was carried out under the guidance of Dr.F.K. Sutaria.

15th August 2011
Bangalore

Chairman
Board of Graduate Studies

ACKNOWLEDGMENT

Success in any endeavor depends a lot on the support, guidance and encouragement received from our guides, friends and parents. The desire to excel and get close to perfection helps us motivate ourselves into giving the best in our means.

I would to express my deep gratitude to my supervisor, Dr. Firoza Sutaria. I would like to thank Dr. Sutaria for her motivation, encouragement and guidance. Her patience and encouragement to analyze failures has definitely made me a better student.

I would like to thank the Board of Graduate Studies for giving me the opportunity to work at the Indian Institute of Astrophysics, Bangalore.

I would also like to thank the faculty, staff and the students at IIA for their cooperation and encouragement. My stay at the Indian Institute of Astrophysics has been a great learning experience.

I would specially like to thank the Department of Physics, Fergusson College, Pune for their support and encouragement. I am grateful to the Head of Department, Dr. D D Choughule for his support.

I am personally indebted to Dr. R V Dabhade for her enthusiasm and encouragement which led me to taking up this project.

I am grateful to all my friends and my parents for their support and encouragement.

I would finally like to thank everyone who has believed in my abilities and more importantly those who have challenged them.

Thanks to this gift of chance, I have been granted a glimpse of the “bigger picture”, a deeply rewarding one.

CONTENTS

Chapter 1

INTRODUCTION

Defocused Photometry is an extremely sensitive method which allows precision photometry with sub-milli magnitude accuracy. The extrasolar planet WASP-12b, in orbit around WASP-12 (G0V), is a 1.41 ± 0.10 M_J gas giant with radius 1.79 ± 0.09 R_J. The high effective temperature of the central star (6300 K) and short orbital period (1.09142 days) make WASP-12b one of the most intensely irradiated extrasolar planets and one of the most well studied ones. The close proximity of the planet to its parent star is pulling away its atmosphere at a rate of about 10^{-7} M_J and has led to bring the surface temperature to more than 2,500 K making it the hottest extrasolar planet. Recent evidence indicates that WASP-12b has a significantly enhanced carbon-to-oxygen ratio, indicating that it is a carbon-rich gas giant.

Our aim was to find the parameters of the Extrasolar Planet "WASP-12b" using transit method. This was done using defocused photometry of WASP-12b transits. Assuming the various limb-darkening laws we generated best-fit models and redetermined the parameters of the system. The photometric error of the individual measurements of the target and reference stars was found to be ranging from 0.3 to 0.4 mmag. Variations are observed in the transit timing. However further observations are needed to confirm these variations.

Chapter 2

THEORETICAL BACKGROUND

"There are countless suns and countless Earths all rotating around their suns in exactly the same way as the eight planets of our system. We see only the suns because they are the largest bodies and are luminous, but their planets remain invisible to us because they are smaller and non-luminous. The countless worlds in the universe are no worse and no less inhabited than our Earth."

- *Giordano Bruno*

Creativity and imagination can be used as synonyms for science. As Christian de Duve from the Institute of Cellular Pathology, correctly puts it, "Science is like any other game of chess or crosswords with an added benefit that it may tell you something about the world".

The realization that our Sun may not be "the only one" or the question "Are we alone?" or the search for extrasolar life was that which led to the search of extrasolar planets or exoplanets. The most encouraging and exciting idea with studying extrasolar planets is that there are at least 200 billion galaxies which contain at least 200 billion stars and hence at least 15 billion giant planets orbiting them.

A "planet" as defined by the International Astronomical Union (IAU) is a celestial body of sufficient mass that is in orbit around the Sun and has cleared the neighbourhood around its orbit. The celestial body which has not cleared the neighbourhood around its orbit, and which is not a satellite is called a dwarf planet and all other objects except satellites orbiting the Sun shall be referred to collectively as "Small Solar System Bodies" . However this definition only covers the Solar System and thus takes no stance on extrasolar planets. An extrasolar planet or exoplanet is a planet orbiting a star or remnant of a star beyond our Solar System. These objects have been defined to have masses less than 13 Jupiter mass with the minimum mass required same as that considered for our solar system. The objects with masses above 13 Jupiter mass are called as brown dwarfs.

The scientific study of extrasolar planets started in the mid-19th Century. There were still many uncertainties as to their discovery, their occurrence and their similarity to our Solar System or how is our Solar System in comparison with planetary systems around other stars. There was also the question of the habitability of such planets. Were there Earth-like planets orbiting other stars and, if so, could they have the necessary surface conditions to support some form of life?

"Extraordinary claims require extraordinary evidence"

The first confirmed detections of extrasolar planets were made in early 1992, by the radio astronomers Aleksander Wolszczan and Dale Frail, but rather surprisingly these were not found around an ordinary star, but a pulsar (PSR B1257+12), the super dense remnant of a massive star that has exploded as a supernova. The first definitive detection of an extrasolar planet orbiting an ordinary main-sequence star came in October 1995 with the announcement, by Michel Mayor and Didier Queloz of the University of Geneva, of an extrasolar planet orbiting the star 51 Pegasi. As of 6th February'2012, 758 extrasolar planets have been identified. In any case, extrasolar planets research has a brilliant future for the next decades and even centuries (assuming that we will last that long).

Chapter 2.1

THE STUDY OF EXTRASOLAR PLANETS

The study of extrasolar planets provides new frontiers to our understanding of the diverse natures of planets, the formation of our Solar System and the possibility of alien life. More than 758 planets have been discovered using different methods of planet detections. Extrasolar planets are distant objects located outside our Solar System, orbiting stars that are far bigger and brighter than the extrasolar planets hence it is very difficult to detect planets using direct imaging. Instead the wobble of the star is studied using Radial Velocity or Doppler method, which is the shift in the wavelength (blue shift or red shift) in the spectrum of visible light from the star. This tiny shift is proportional to the mass ratio. Stars wobbles are also studied with respect to the other stars which is known as astrometry. Gravitational microlensing is another method which uses Einstein's theory of bending of light where the light from a background star will bend due to a foreground star. Transiting method is by far the most useful method of extrasolar planet detection as it exploits the least daunting inequality between the star and the orbiting planet. As the planet transits the star i.e. passes across the disk of its parent star, there is a fall in the intensity of the stars light by a fraction of $(R_P/R_S)^2$ where R_P and R_S are the radii of planet and star respectively. Though it is a fruitful method, transits can be observed only when the planets orbit is almost edge-on when the star is observed, which is extremely unlikely. Also despite of the accuracy of Transit methods, most of the planets found so far have much less density than predicted. The abundance of less dense planets is difficult to explain through theoretical models. Most of the extrasolar planets found have masses ranging from 0.5 to 3 Jupiter mass and radii ranging from 0.8 to 1.7 times that of Jupiter's radius. Jupiter has a small core of heavy elements, surrounded by hydrogen with some helium content. An extrasolar planet with the mass almost equal to that of Jupiter's but a smaller size (higher mean density) probably may have a larger core with more heavy elements but for extrasolar planets with smaller density even the planet made up of only hydrogen does not explain its low density satisfactorily. One possible reason could be the additional heating of the planet due to its parent star in case of extremely close orbits or a delay in the cooling of the planet but then there still remains an unanswered question as to why only

some planets would absorb the heat and the others would not. All these methods help to study the different parameters of the planet.

The Doppler technique gives the size, eccentricity, period and Msin*i* (where Msin*i* gives the lower limit of the planet's mass and is not the actual mass). By studying the fall in intensity parameters like radius of the planet and the orbital inclination angle (*i*) can be calculated. Combining the inclination angle and Msini, the mass of the planet and hence its mean density can be calculated. Apart from the physical parameters basic spectroscopy and thermal mapping help in studying the planetary atmosphere. Presence of water is very common in low temperature environments owing to the abundance of hydrogen and oxygen or the presence of carbon dioxide and methane but since very little is known about the upper atmospheres it is difficult to detect the presence of water. Water has already been seen on 3 hot Jupiter's; TrES-1, HD 209458 b and HD 189733 b. The terrestrial planets (Super Earths) discovered so far have their masses ranging from 5 to 10 Earth masses. Astronomers generally expect a great diversity among smaller planets because smaller, solid planets depending on the compression, cooling and mixing of their material as also on their weight and interior can have more varied material compositions. Depending on the dominance of iron or iron-alloy, silicate mantle, ice (mostly water), hydrogen-helium envelope or carbon rich mantle there are two distinct types, the ocean planets (with water making up more than 10% of their mass) and rocky, Earth-like planets (water makes up only about 0.05% of Earth by mass but they may still have oceans). Our own solar system has a variety of rocky planets and gas giants. There still remains the most interesting question to be answered, which is that of the presence of another Earth and if it would be present, then if it would necessarily be habitable. With the advances in technology, spectroscopy would help detect Earth like planets and the transit studies and theoretical models with respect to the Earth would help find the habitability of these planets. (Dimitar D Sasselov, 2008).

"There are infinite worlds both like and unlike this world of ours... We must believe that in all worlds there are living creatures and plants and other things we see in this world."

- Epicurius

Chapter 2.2

SPACE MISSIONS FOR THE DETECTION AND STUDY OF EXTRASOLAR PLANETS

Current:

- MOST - The **Microvariability and Oscillations of STars** telescope, launched in 2003, is Canada's first space telescope dedicated to the study of astroseismology.
- COROT – COnvection ROtation and planetary Transits, launched in 2006, is the first spacecraft dedicated to extrasolar planet detections led by the French Space Agency (CNES) in conjunction with the European Space Agency (ESA) and other international partners. The mission's two objectives are to search for extrasolar planets with short orbital periods, particularly those of large terrestrial size, and to perform astroseismology by measuring solar-like oscillations in stars.
- Kepler Mission – The Kepler Mission, launched in 2009, is specifically designed to survey a portion of our region of the Milky Way galaxy to discover dozens of Earth-size planets in or near the habitable zone and determine how many of the billions of stars in our galaxy have such planets. Kepler uses a photoelectric photometer developed by NASA to continuously monitor the brightness of over 145,000 main sequence stars in a fixed field of view. During the period of May to September 2009 the Kepler team found 1235 planetary candidates circling 997 host stars, more than twice the number of currently known extrasolar planets. The Kepler results included 68 planetary candidates of Earth-like size and 54 planetary candidates in the habitable zone of their star. The team estimated that 5.4% of stars host Earth-size planet candidates and 17% of all stars have multiple planets.

Under development:

- Gaia mission – Global Astrometric Interferometer for Astrophysics, launch in March 2013 is a European Space Agency (ESA) astrometry space mission, and a successor to the ESA Hipparcos mission. Gaia will compile a catalogue of approximately one billion stars to magnitude 20. Its objectives comprise the astrometric (or positional) measurements, determining the positions, distances, and annual proper motions of stars with an accuracy of about 20 μas (microarcsecond) at 15 mag, and 200 μas at 20 mag, spectrophotometric measurements, providing multi-epoch observations of each detected object and radial velocity measurements.

Proposed:

- PEGASE – PEGASE is a proposed space mission to build a double-aperture interferometer composed of three free-flying satellites. The goal of the mission is the study of Hot Jupiter's (pegasids), brown dwarfs and the interior of protoplanetary disks. The mission would be performed by the Centre National d'Études Spatiales and is currently being studied for launch around 2010–2012.
- TESS – Transiting Exoplanet Survey Satellite (TESS) is a proposed space telescope by MIT for NASA's Small Explorer program. The survey would focus the G and K spectral type stars brighter than 12 magnitudes, approximately 2 million of them would be studied, and the 1,000 closest M-type red dwarfs (within 30 parsecs). It is expected to discover 1,000 - 10,000 transiting extrasolar planets down to the size of the Earth and up to 2 months of period. The candidates could be later investigated by the HARPS spectrometer and some of them could be targets of the James Webb Space Telescope.

- New Worlds Mission – The New Worlds Mission, launch in 2014 is a project funded by NASA Institute for Advanced Concepts (NIAC).The project plans to build a large occulter in space designed to block the light of nearby stars in order to observe their orbiting planets. The observations could be taken with an existing space telescope, possibly the James Webb Space Telescope when it launches, or a dedicated visible light telescope optimally designed for the task of finding extrasolar planets.
- PLATO – PLAnetary Transits and Oscillations of stars (PLATO) is a European Space Agency-proposed space observatory that will use a group of photometers to discover and characterize extrasolar planets of all sizes and kinds around cool dwarf (like our Sun) and sub giant stars. The satellite is planned to be launched in 2017 or 2018. It will differ from COROT and the Kepler Mission in that it will study relatively bright stars (between magnitudes 8 and 11) making it easier to confirm discoveries using follow-up radial velocity measurements.
- EChO - The Exoplanet Characterisation Observatory (EChO) is a proposed space telescope that has been selected for further studies as part of the Cosmic Vision roadmap of the European Space Agency. EChO will be the first dedicated mission to investigate exoplanetary atmospheres, addressing the suitability of those planets for life and placing our Solar System in context. EChO will provide high resolution, multi-wavelength spectroscopic observations. It will measure the atmospheric composition, temperature and albedo of a representative sample of known extrasolar planets, constrain models of their internal structure and improve our understanding of how planets form and evolve. It will orbit around the L2 Lagrange point, 1.5 million km from Earth in the anti-sunward direction.

Chapter 2.3

METHODS OF DETECTING EXTRASOLAR PLANETS

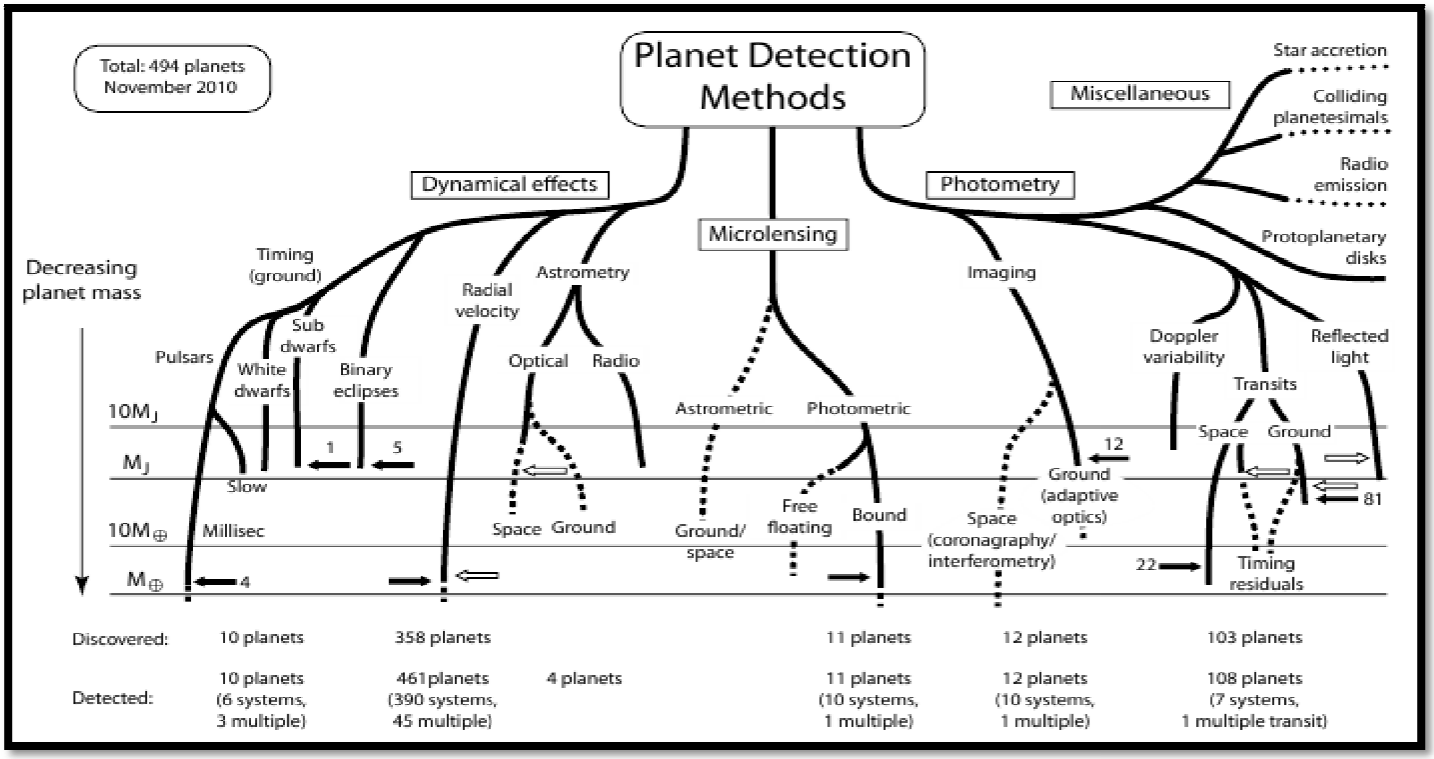

Figure 2.1 : The above chart lists the different methods used for detection of Extrasolar Planets.

There are a number of ways of detecting the existence of extrasolar planets, most indirect. All the techniques have their own advantages and disadvantages. Currently employed detection methods are biased towards close-orbiting heavy planets and thus very few lighter terrestrial-like planets have so far been found, with the lowest mass for planet orbiting an active star so far being estimated as $5.5M_{Earth}$. Planets are extremely faint light sources compared to their parent stars. At visible wavelengths, they usually have less than a millionth of their parent star's brightness. It is difficult to detect such a faint light source, and furthermore the parent star causes a glare that tends to wash it out. Directly observing extrasolar planets is extremely difficult given the large brightness contrast between a star and its planets and also the small angular separation. For the above reasons, telescopes have directly imaged no more than about ten extrasolar planets. This has only been possible for planets that are especially large (usually much larger than Jupiter) and widely separated from their parent star. Most of the directly imaged planets have also been very hot, so that they emit intense infrared radiation; the images have then been made at infrared rather than visible wavelengths, in order to reduce the problem of glare from the parent star.

Chapter 2.3.1

RADIAL VELOCITY OR DOPPLER METHOD

As a planet orbits a star, the star also moves in its own small orbit around the system's center of mass. Variations in the star's radial velocity (i.e. the speed with which it moves towards or away from Earth) can be detected from displacements in the star's spectral lines due to the Doppler Effect. Extremely small radial-velocity variations can be observed, down to roughly 1 m/s. This has been by far the most productive method of discovering extrasolar planets. It has the advantage of being applicable to stars with a wide range of characteristics.

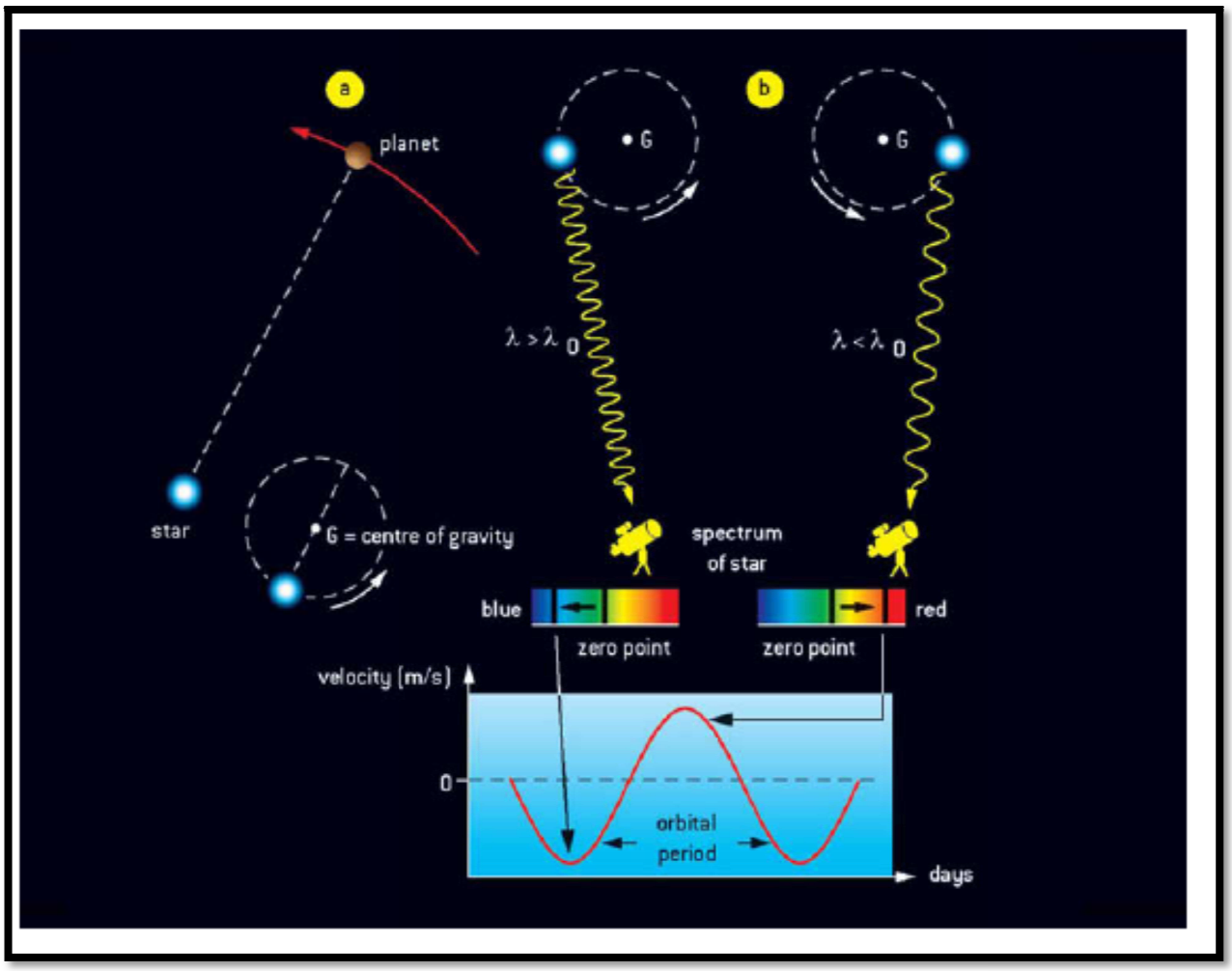

Figure 2.2 : The above figure shows the Doppler (red and blue shift) or Radial Velocity method for detecting extrasolar planets. The spectrum is blue shifted if the planet comes towards the observer and red shifted when it goes away from the observer.

The presence of a planet causes a variation in the radial velocity of a star. This depends on several criteria: the mass of the star, the mass of the planet, the period of the planet's orbit (P), and the orbital eccentricity. Variations in velocity due to a planet in a circular orbit are sinusoidal, with a period matching the orbital period P of the planet. Their amplitude K in m/s is expressed by

$$K = 28.4\ P^{-1/3}\ (M_P \sin i)\ M^{*\,-2/3}$$

It should be noted that it is not the mass of the planet which is directly involved, but the quantity $M_P \sin i$, where the angle *i* defines the inclination of the orbit of the planet as seen from Earth. If this angle is 90° with respect to the plane of the sky, the orbit is seen edge-on. In this case, sin *i* is 1, and the variation in velocity is maximized. If the angle is 0°, then the orbit is seen face-on, and sin *i* is 0, causing no variation in radial velocity. Usually angle *i* is between 0° and 90°, and $M_P \sin i$ lies between 0 and the actual value of the mass of the planet.

As there is no other source of information than the measurement of radial velocities, neither the inclination of the orbit nor the value of sin *i* are known. Hence it can be used to determine the minimum value of that mass and not the actual mass. The parameters obtained are therefore the minimum mass, the period (directly linked with the semi major axis (a) of the orbit, according to Kepler's third law $T^2 \alpha a^3$), and the eccentricity of the orbit if not circular. The first confirmed discovery of an extrasolar planet (51 Pegasi b) was made using this method. The velocimetric method is therefore well suited to the study of massive, short-period planets, close to their stars; in short, 'hot Jupiter's'. As of 6th February'2012, 557 planetary systems have been discovered using this method including 92 multi planet systems.

Chapter 2.3.2

TRANSIT METHOD

From immemorial antiquity, men have dreamed of a royal road to success—leading directly and easily to some goal that could be reached otherwise only by long approaches and with weary toil. Times beyond number, this dream has proved to be a delusion.... Nevertheless, there are ways of approach to unknown territory which lead surprisingly far, and repay their followers richly. There is probably no better example of this than eclipses of heavenly bodies.

- Henry Norris Russell (1948)

If a planet crosses (or transits) in front of its parent star's disk, then the observed brightness of the star drops by a small amount. The amount by which the star dims depends on its size and on the size of the planet, among other factors. This has been the second most productive method of detection, though it suffers from a substantial rate of false positives and confirmation from another method is usually considered necessary.

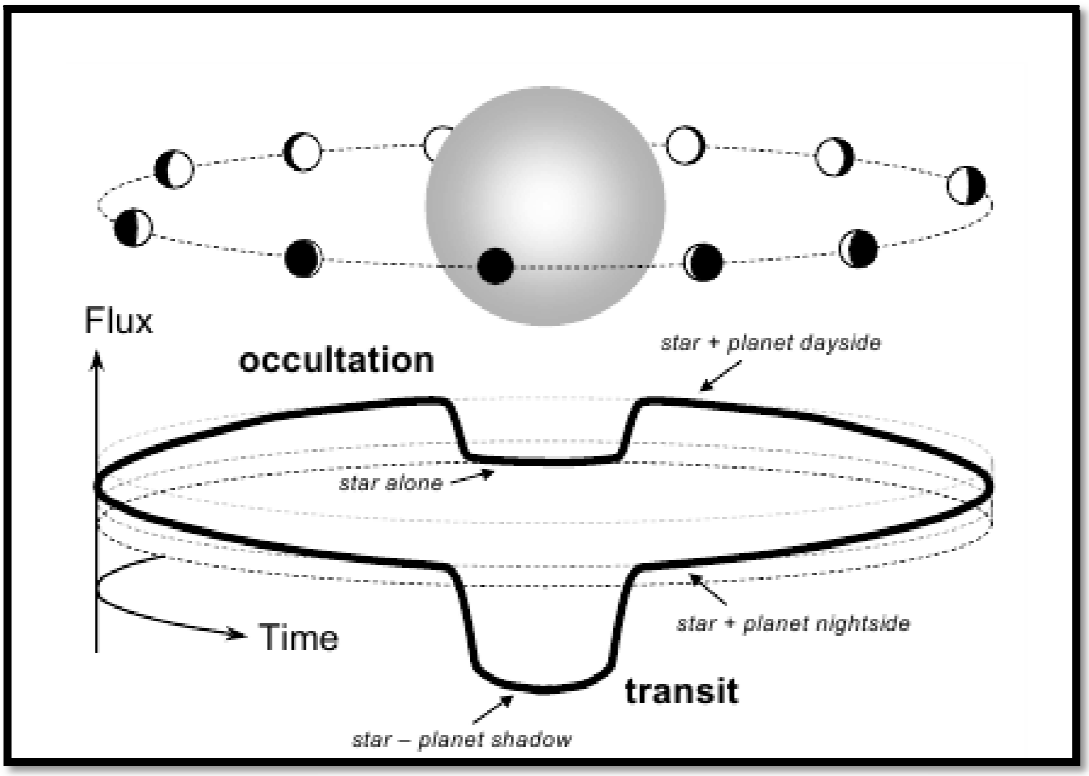

Figure 2.3 : The above figure shows the transit and occultation of a planet orbiting a star measured with respect to the flux and time.

If the star were indeed a point source, the transit would occur only if the star, the planet and the observer were in exact alignment. However, since the star has a definite radius R^*, calculation shows that the probability of transit is expressed by R^*/ a, where a is the orbital radius. The probability of having a transit can be computed from the inclination of the orbit with respect to the observer. The inclination angle (i) and the latitude of trajectory ( ) are equivalent. The nearer a planet is to its star, the greater the possibility of a transit; and the larger the star, the greater the chance that the planet will be seen to pass across it. The diminution in brightness is simply the ratio of the apparent surfaces of the planet and the star,

$$\Delta F = (R_P/R^*)^2$$

where R_P is the radius of the planet and R^* is the radius of the star.

Hence, if we are able to estimate the radius of the star we can deduce the radius of the planet. The duration of the transit depends firstly upon the period of revolution of the planet around the star (the further away the planet is from the star, the longer it will take to pass across its face), and secondly, upon the inclination of the orbit. For planets at different distances, the transit may last for periods ranging from hours to several days.

$$\tau = \frac{P}{\pi}\left(\frac{R_s \cos\delta + R_p}{a}\right)$$

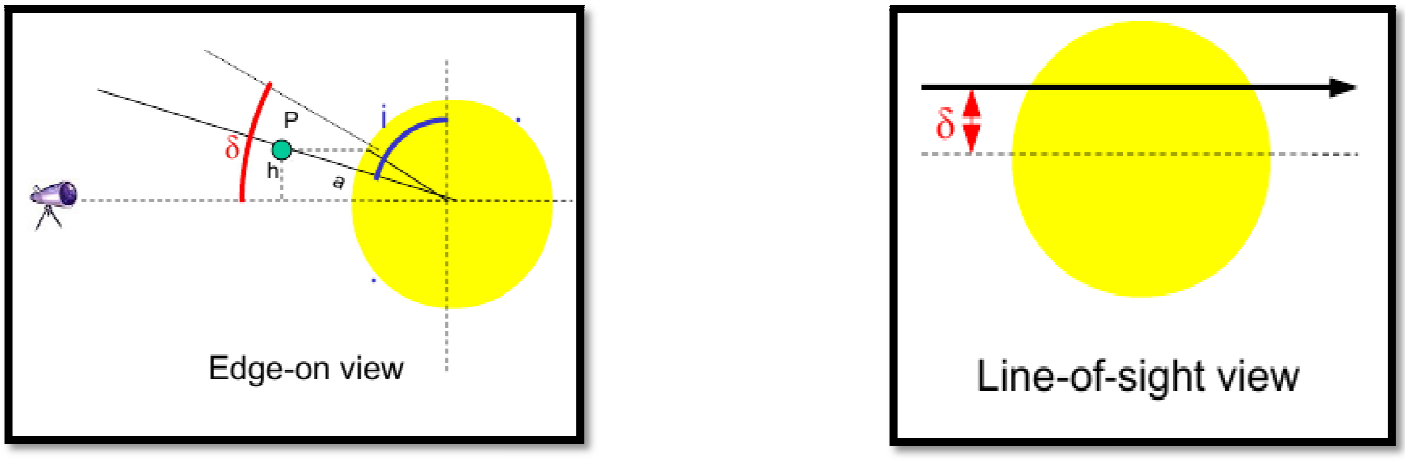

Figure 2.4 : Edge on view and Line of sight view

In the final analysis, from transit observations we can deduce the radius of the planet, its period, the inclination of its orbit and hence its mass, using the minimum mass Msini obtained via radial velocity method. With mass, radius and distance from its star all known, some physical studies can be undertaken. The existence of transiting planets allows many useful measurements. The reason is that the planet can be observed in the combined light of the planet-star system, so that although the planet and star are not separated in space as viewed from a telescope, the brightness of the planet and star can be separated from each other. As of 6th February'2012, 195 planetary systems have been discovered using this method including 29 multi planet systems.

TRANSIT TIMING VARIATION:

Transit Timing Variation (TTV) is a variation on the transit method where the variations in transit of one planet can be used to detect another. The new method can potentially detect Earth sized planets or exomoons. For a given transiting planet the TTV depends on 7 unknown parameters of the perturbing planet i.e. its mass, semi-major axis, eccentricity, inclination, nodal and periapse longitudes and difference of mean orbital phases of both planets for a given epoch.
A mean motion resonance is a dynamic relationship between two objects orbiting the same primary, such that the ratio of their orbital periods can be expressed by two small integers; e.g., 2:1, 3:1, 4:1, 3:2, or 4:3. The principle of Mean motion resonance can be used to detect multi-planet systems. A terrestrial mass planet perturbing a hot-Jupiter gas giant is expected to cause a TTV amplitude of ~1 minute (depending on the distance) and this signal grows sharply as bodies approach a mean motion resonance. With the help of the amplitude of the TTV, which may be treated as a minimal value, one can determine the minimal mass of the additional planet in a wide range of orbital configurations.

Chapter 2.3.3

GRAVITATIONAL MICROLENSING

Gravitational microlensing provides a unique window on the properties and occurrence of extrasolar planetary systems because of its ability to find low-mass planets at separations of a few AU. The early evidence from microlensing indicates that the most common types of extrasolar planets yet detected are the so-called super-Earth planets of 10 Earth masses at a separation of a few AU from their host stars .Microlensing occurs when the gravitational field of a star acts like a lens, magnifying the light of a distant background star. Planets orbiting the lensing star can cause detectable anomalies in the magnification as it varies over time. This method has resulted in only a few planetary detections, but it has the advantage of being especially sensitive to planets at large separations from their parent stars.

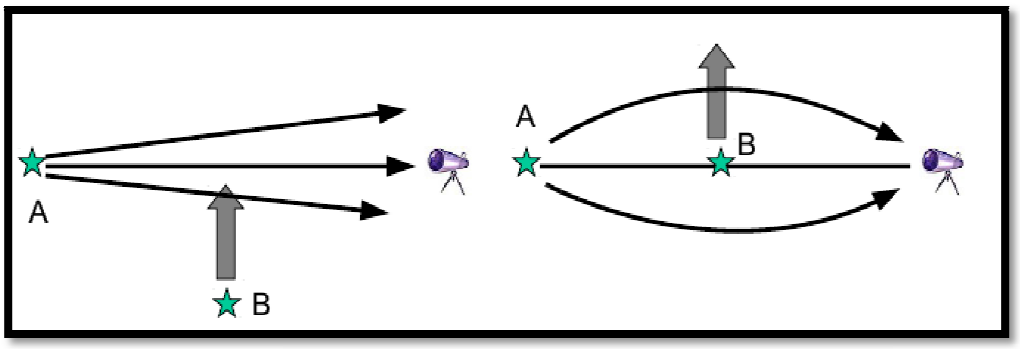

Figure 2.5 : The above figure shows the effect of microlensing in star system.

The gravitational microlensing method relies upon chance alignments between background source stars and foreground stars, which may host planet systems. These background source stars serve as sources of light that are used to probe the gravitational field of the foreground stars and any planets that they might host. The relative motion of the source star and lens system allows provides the observable gravitational microlensing signal. Microlensing effects can also be detected in case of a planet-star system. The microlensing method is unique among extrasolar planets detection methods in a number of respects:

1) There is more than 10% increase in the stellar luminosity due to planetary microlensing and is approximately independent of the planetary mass. Instead, the source-lens alignment

necessary to give a detectable planetary signal depends on the planet- star mass ratio, q, and so the probability of a detectable planetary signal scales as ≈ q.

2) This scaling of the probability of planet detection with the mass ratio, q, is shallower than the sensitivity curves for other methods, so microlensing is more sensitive to low-mass planets than other methods that are sensitive to planetary mass. The sensitivity of the microlensing planet search method extends down to $0.1M_{\oplus}$.
3) Microlensing is most sensitive to planets at orbital separations of 1.5-4 AU (1 AU = 1.49×10^{13} cm), which corresponds to the vicinity of the Einstein ring radius. Thus, microlensing complements the Doppler radial velocity and transit methods, which are most sensitive to planets in very short period orbits.
4) Microlensing is the only planet detection method that is sensitive to old, free floating planets, which have been ejected from the gravitational potential well of their parent stars through planet-planet scattering as it does not rely on the light from the lens star. Theory predicts that such planets may be quite common, and ground-based microlensing can detect free floating gas giant planets, while a space-based survey is needed to detect free floating terrestrial planets.
5) Since the microlensing method doesn't rely upon light from the host star in order to detect its planets, it can detect planets orbiting unseen stars. This can make it difficult to determine the properties of the host stars, but space-based follow-up observations can detect the host stars for most planets discovered by microlensing.
6) A space-based microlensing survey would provide a nearly complete statistical census of extrasolar planets with masses down to $0.1M_{\oplus}$ at all separations $\geq$ 0.5AU.

Gravitational microlensing differs from other extrasolar planet search techniques in a number of aspects. It is a purely gravitational method that doesn't rely upon on detecting photons from either the planet or its host star. While most of the known extrasolar planets have been discovered with the Doppler radial velocity method, the early results from the microlensing method indicate that cool; super-Earth or sub-Neptune mass planets are more representative of typical extrasolar planets than any of the 200+ extrasolar planets discovered by radial velocities.

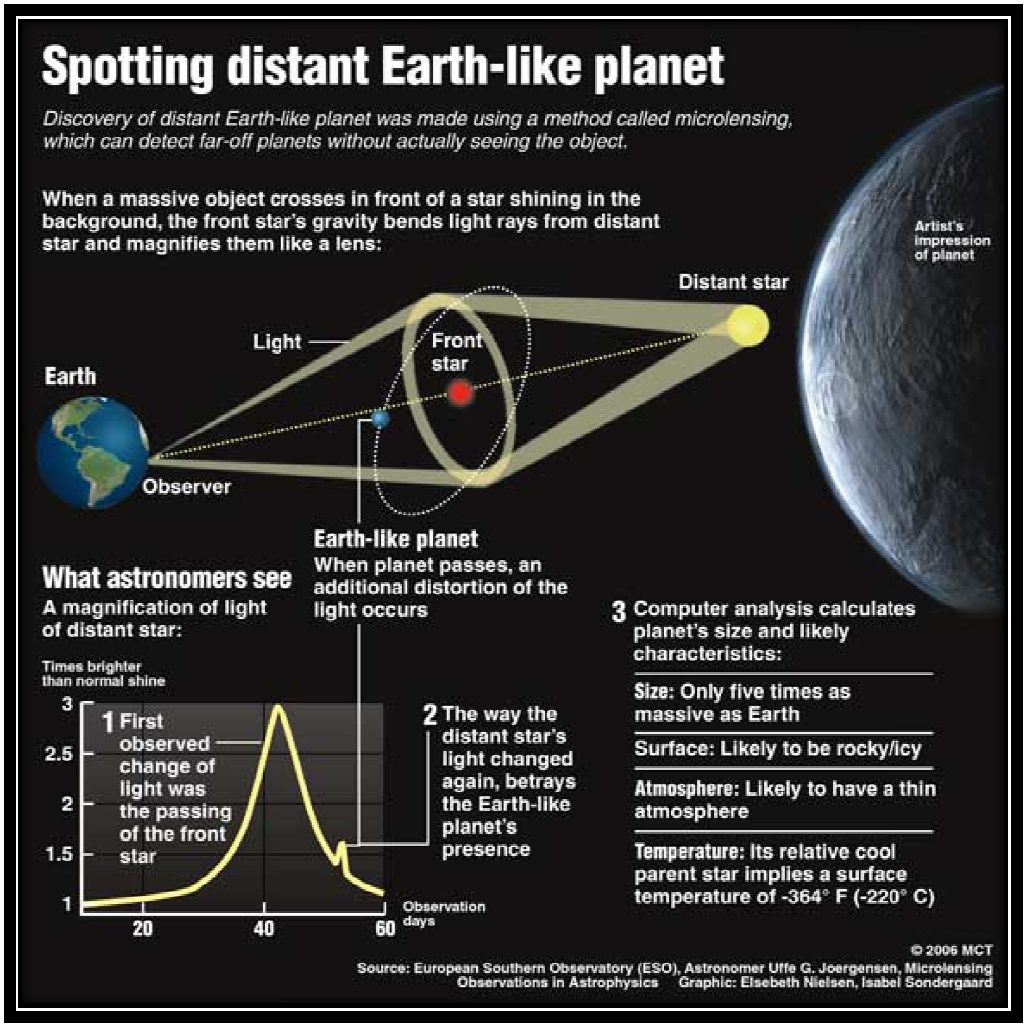

Figure 2.6 : The figure above gives details of Microlensing

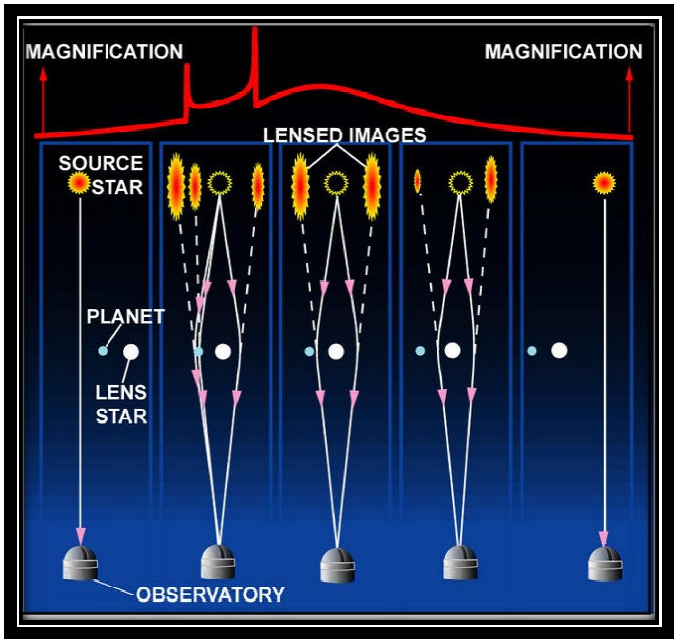

Figure 2.7 : The above figure shows the effect of change in the alignment of the background star and the foreground star.

Chapter 2.3.4

ASTROMETRY

Astrometry consists of precisely measuring a star's position in the sky and observing the changes in that position over time. Given a sequence of observations of a star's position of sufficiently high accuracy relative to the celestial sphere, the reflex motion of the star due to the gravitational influence caused by the orbit of a planet around it can be detected. This can be used to determine both the absolute mass and orbital inclination of a planet. Considering the motion of the star and planet about their common centre of mass we can see that the reflex amplitude of the star is

$$a^* = a_P M_P / M^*$$

where a^* and a_P are the distances from the centre-of-mass to the star and planet respectively. Thus, this method is most effective for large mass planets orbiting at some distance from their parent stars. This method is best for planetary systems within a few parsecs of the Earth as angular position of the star is measured.

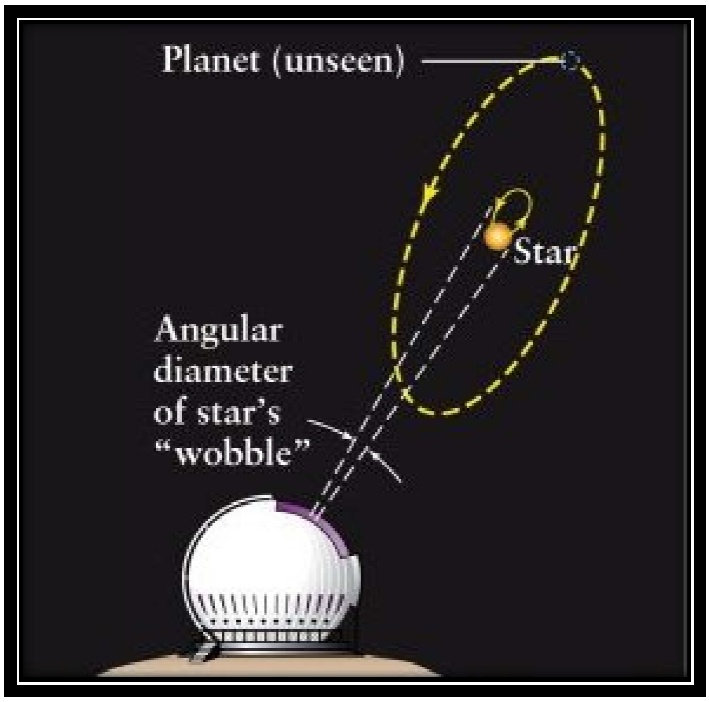

Figure 2.8 : The above figure shows the stars wobble due to an orbiting planet

To improve the accuracy of astrometric measurements, interferometry is used, which uses the combined signals from a number of telescopes to synthesize images at very high angular resolution. Very-long-baseline interferometry (VLBI) can achieve angular resolutions of the order of 0.1 milliarcseconds. However, this is restricted to very intense radio sources, and the possible range of targets is considerably reduced. We must therefore look to the interferometers of the future, working in the visible and near-infrared. The interferometer of the Large Binocular Telescope (LBT), consisting of two telescopes on the same mounting, should be able to achieve a resolution of the order of 0.1 milliarcseconds.

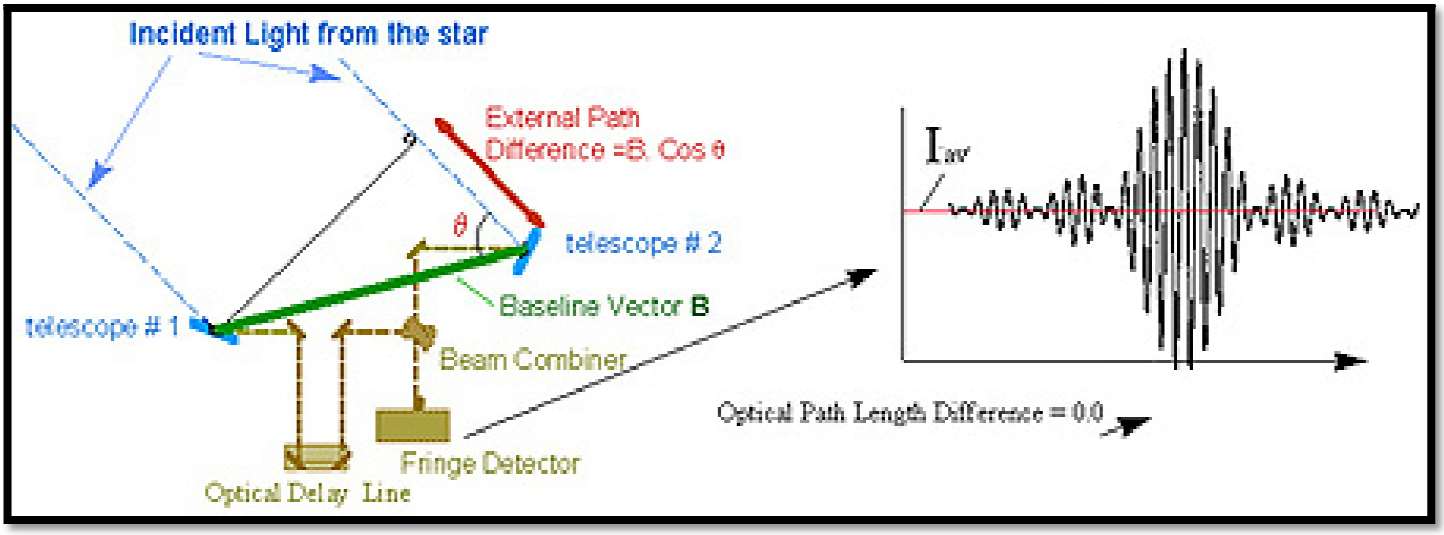

Figure 2.9 : The above figure describes the method of Astrometric Interferometry

Chapter 2.3.5

PULSAR TIMING

A pulsar (the small, ultra dense remnant of a star that has exploded as a supernova) emits radio waves extremely regularly as it rotates. If planets orbit the pulsar, they will cause slight variations in the timing of its observed radio pulses. As the planet orbits the pulsar, its small but finite mass causes the pulsar to undergo a tiny reflex orbit about the center of mass of the pulsar-planet system. Planets detected by this method have orbits ranging from ≈ 0.19 AU (PSR B1257+12 b) to 23 AU (PSR B1620-26 b). The pulsar orbits the system's center of mass with an orbital radius smaller by a factor equal to the ratio of the mass of the planet to that of the pulsar. (According to Kepler's third law – $P^2/a^3 = 4\pi^2/MG$). Since the pulse arrival time is measurable to a precision of a microsecond and less, the periodic change in arrival time can be easily measured. Pulsar timing is the most sensitive method for detecting pulsar planets. It involves the study of variations in the pulsar's period, expressed in milliseconds. Since this method is extremely precise, tiny variations in the period can be detected. By this method, even 'exoMoons' are detectable. Note that the sensitivity of this method does not explicitly depend upon the distance of the pulsar. However, difficulties remain, as the signals from more distant pulsars are weak, and timings of them are less accurate. This method can also be used for detecting planets around any star from which the signal has a periodic profile (e.g. UZ For(ab) c which is an eclipsing binary, NN Ser (ab) which is a white dwarf +M binary).The first confirmed detections of extrasolar planets found orbiting the pulsar (PSR B1257+12), using this method were made in early 1992, by the radio astronomers Aleksander Wolszczan and Dale Frail.

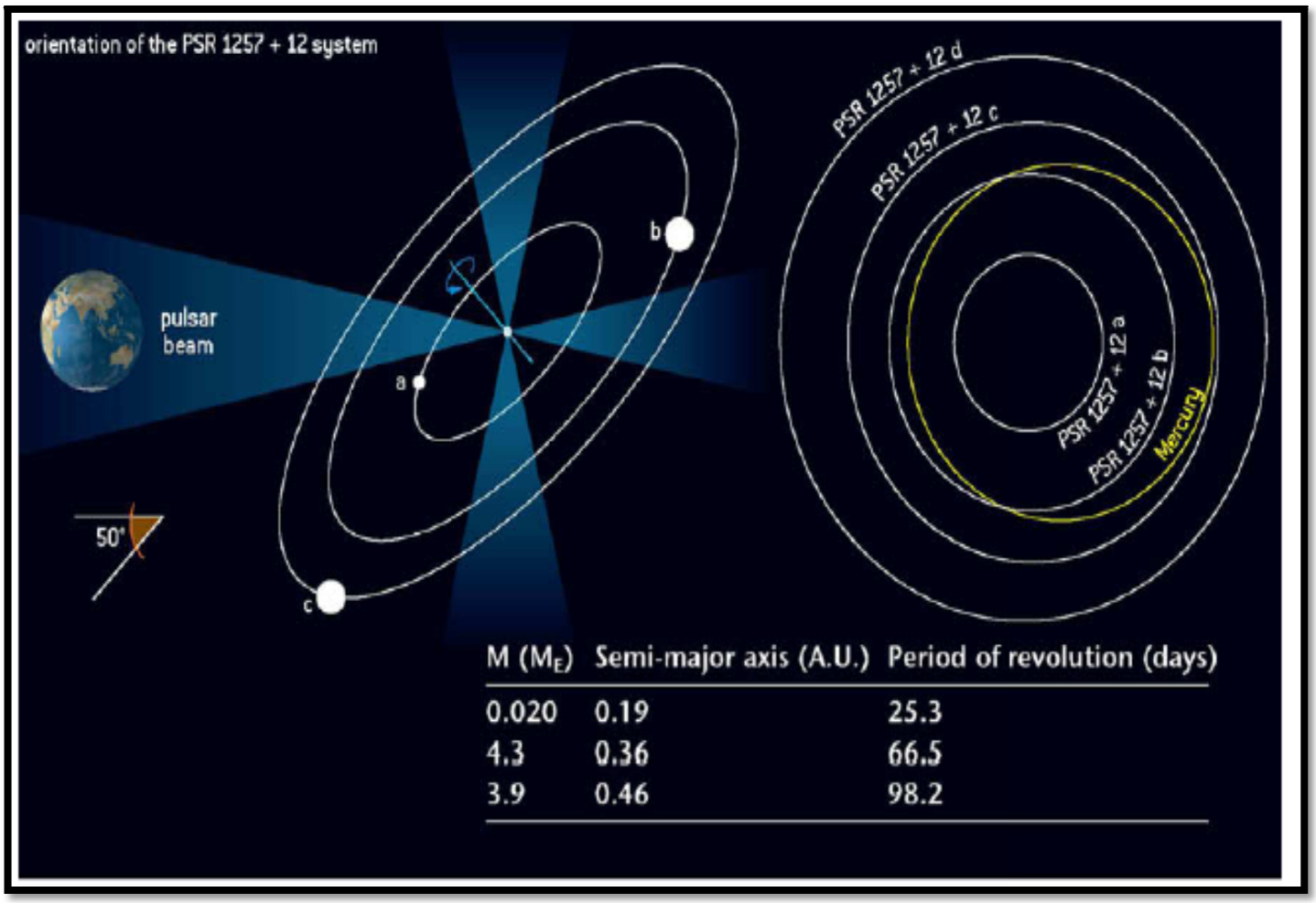

Figure 2.10 : The above figure explains the Pulsar timing method of detection of extrasolar planets. It shows a multi-planet system orbiting the pulsar – PSR 1257+12 and gives the basic parameters of mass of the planets with respect to the mass of the earth, the semi-major axis in AU and also the period of revolution in days.

Chapter 2.4

WIDE ANGLE SEARCH FOR PLANETS
SuperWASP

There are an estimated 10 billion planetary systems in our galaxy alone, yet to-date, only a few hundred have been discovered. Extrasolar planets are very difficult to detect because they don't emit any light of their own and are completely obscured by their extremely bright parent stars. Normal telescope observation techniques cannot be used. Instead of trying to image/detect extrasolar planets directly SuperWASP looks for the physical effects they have on their parent star such as shifts in position or changes in brightness.

SuperWASP is the UK's leading extra-solar planet detection program comprising of a consortium of eight academic institutions which include Cambridge University, the Instituto de Astrofisica de Canarias, the Isaac Newton Group of telescopes, Keele University, Leicester University, the Open University, Queen's University Belfast and St. Andrew's University. SuperWASP consists of two robotic observatories that operate continuously all year around, allowing us to cover both hemispheres of the sky. The first, SuperWASP-North is located on the island of La Palma amongst the Isaac Newton Group of telescopes (ING). The second, SuperWASP-South is located at the site of the South African Astronomical Observatory (SAAO), just outside Sutherland, South Africa.

SuperWASP detects planets by looking for 'transits'. These occur when a planet passes in front of its parent star, temporarily obscuring some of its light. This can be detected from the Earth as a slight dimming of the star's luminosity. The dimming can be as little as 1% so extremely accurate measurements are needed. As the planet passes in front of the star it produces a characteristic 'light-curve' whose shape is affected by the size and orbital distance (and hence orbital period) of the planet. The eight wide-angle cameras allow us to monitor millions of stars simultaneously enabling us to detect the rare transit events. SuperWASP constantly monitors the brightness of the stars in its field of view and detects any variations that may be due to the presence of a planet. The SuperWASP observatories each consist of an array of 8 cameras with an aperture of 11.1 cm, backed with a high-quality CCD. These cameras are extremely wide field - up to 2000 times greater than a conventional astronomical telescope.

The cameras continuously image the night sky, each camera capturing up to 100,000 stars per image (this many are needed to stand any chance of detecting transiting planets). This amounts to over 50 gigabytes of observational data per night, per observatory, which is automatically processed by our custom built computer 'Pipeline'.

The 'Pipeline' first reduces the images by removing errors such as variations in pixel sensitivity, dirt/scratches on the lenses, noise etc. This is done by comparing the images to special calibration images. The diagram below shows three of these images;

1) 'Flat-field' - an image (or several images) of a uniform area of the sky taken at twilight, used to remove variations in pixel sensitivity across the CCD, dust and scratches and variations in illumination across the lens known as vignetting.
2) 'Bias' - a short exposure image with the lens shutter in place, used to estimate the effect of a voltage difference applied to the CCD to ensure a linear response.
3) 'Dark-current' - a longer exposure with the lens shutter in place, used to eliminate thermal noise from the CCD (although the CCDs are cooled to -50C thermal noise is still present).

The 'pipeline' then examines the images and matches each star with an astronomical catalogue of stars to identify them. Finally a complex photometric analysis is performed to measure the brightness of every star, the results of which are stored in the project database hosted by the University of Leicester. When sufficient observations have been made (over several months), we perform searches for dips in brightness that might indicate the presence of a planet passing in front of a star. Unfortunately there are a large number of phenomena, other than planets, that can cause changes in stellar brightness. Very careful analysis is needed to verify the presence of a planet which is performed by the Geneva Planet Search group. To confirm the presence of the planet they use sensitive spectrographs to measure the minute shift in position of the star as the planet orbits around. Once confirmed, astronomers can then use large instruments such as the Hubble and Spitzer space telescopes to study these worlds. As of 13th April, 2010 around 33 planets have been detected by SuperWASP using transit method.

Chapter 2.5

HIMALAYAN CHANDRA TELESCOPE HANLE, INDIA

A 2-m aperture optical-infrared telescope, the Himalayan Chandra Telescope (HCT) manufactured by the EOS Technologies Inc., Tuscon, Arizona, USA is installed at IAO. The telescope is remotely operated from CREST, Hosakote, via a dedicated satellite link. The telescope is equipped with 3 science instruments which are mounted on an instrument mount cube at the cassegrain focus of the telescope. The instrument mount cube has four side ports and an on-axis port, which makes all three instruments available mounted on the telescope. The instruments currently available are the Himalaya Faint Object Spectrograph (HFOSC), the near-IR imager, and the optical CCD imager. The telescope tracking tests indicate that a tracking accuracy (without guiding) of 0.5 arcsec over 10 minutes is met at a good fraction of telescope positions, except at higher elevations, where the tracking worsens, resulting in a mean (over all telescope positions) accuracy of 1.38 arcsec over 10 minutes. A pointing accuracy of 3 arc seconds has been achieved. The image quality is estimated to be about 0.7 arc seconds diameter (80% power). The autoguider (AUGUS) developed at the Copenhagen University Observatory was installed in May 2005. The AUGUS has been performing well, reaching 17 mag stars in 4 second integration.

Table I

Aperture	2.01 meters
Optics	Ritchey-Chretien
Mount	Altitude over azimuth
Focus	Cassegrain; provision for Nasmyth
F-ratio	f/1.75 primary; f/9 Cassegrain
Plate Scale (HFOSC)	0.296 arcsec/pixel
Image Scale	11.5 arcsec/mm
Field of View	7 arcmin; 30arcmin with corrector

Figure 2.11 : 2m- Himalayan Chandra Telescope, Hanle, India

Chapter 2.6

CHARGED COUPLE DEVICE

- Basic Principle:

The CCD is a semi-conductor device designed to detect extremely faint objects. A CCD is essentially an array of light sensitive elements. These elements are arranged in a grid, and each is referred to as a pixel. A typical modern CCD may have 2048×2048 pixels, just over 4 million in total. The pixels are typically 15 to 25 microns in size. CCDs work by converting photons into electrons which are then stored in each pixel. Each pixel can hold a fixed maximum number of electrons, typically from 35,000 to as many as 500,000. A photon hitting a pixel knocks loose an electron, and hence deposits a charge on the pixel. The charge on each pixel is thus a measure of the number of photons which strike it. The number of photons striking the CCD is called the quantum efficiency (QE) of the device. The QE of the best photographic film is only about 1% and that of a CCD which is wavelength dependent is about 90% in the optical. The extremely high QE of CCDs is why they are so much better than photographic film. CCDs have another great advantage over photographic film: linear response. Also, the images produced by CCDs are digital, which allows one to analyze CCD data more directly on a computer. After an exposure has been completed, the electrons for each pixel are shifted out of the CCD and converted to a number, indicating how dark or light each particular pixel should be, and stored in the image file.

- Sources of noise in CCD images and their elimination:

Every photon striking a pixel would be converted into exactly one electron. Then the number of electrons would be precisely counted and converted to a number telling exactly how much light struck each pixel. The processes of converting light to pixel values in a CCD image introduce "noise" into an image. Noise is unwanted variations in pixel values that make the image a less than exact representation of the original scene. Reducing the noise can give you a better Signal-to-noise ratio. There are several different sources of noise that are introduced during the

integration and read out of an image from a CCD. CCD manufacturer's measure and report CCD noise as a number of electrons RMS (Root Mean Square).

(1) Dark Current: The signal recorded at each pixel on a CCD may, in some cases, have an additional component which has nothing to do with the number of photons which struck it. This extra charge deposited in pixels is due to the heat in the material of the CCD (due to motion of atoms).This is known as "Dark Current". To reduce this effect, all CCDs used in astronomy are cooled to very low temperatures. The best CCDs are cooled with liquid nitrogen to about -110_C, and have negligible dark current. The rate of dark current build up can be reduced by a factor of 100 or more by cooling the CCD. The remaining dark current is subtracted from an image using dark frames. Dark frames can be acquired by taking an exposure of same duration as that of the other frames by keeping the CCD shutter closed. Dark Current is time and temperature dependent.

(2) Pixel Non-Uniformity: Each pixel has a slightly different sensitivity to light, typically within 1% to 2% of the average signal. This variation may be because the optics of the telescope may not transmit light uniformly across the entire field of view or the presence of dust on the CCD itself or the glass CCD cover (this typically appears as broad dark rings on the image). Also the QE of individual pixels varies across the CCD, causing a variation in sensitivity. To correct for this effect, one must acquire flat-field images. This requires a source of even illumination usually either a diffusing screen and a light within the telescope dome itself, or the twilight sky. Flat fields taken with a dome diffusing screen are known as 'dome flats' and those taken using the twilight sky as the illumination source are known as 'sky flats'. Several flats should be taken to allow for the construction of a master flat, and a separate master flat must be constructed for each filter used. The flat field correction is made with this master flat field, by dividing the image to be corrected by the flat field. The individual flat field images should be over scan corrected, trimmed, de-biased and corrected for dark current effects prior to combining.

(3) CCD Noise: A pixel value is read out of a CCD as a tiny voltage, on the order of microvolts per electron. This voltage is then converted into digital pixel value and during this process there are a lot of chances of introducing additional noise into the CCD image. The values of the pixels on a CCD image of zero duration are considered to consist of three components. There are extra pixels generated by the CCD electronics when the CCD is read out. They are not in any way connected to real physical pixels on the CCD; they correspond to locations on the pixel grid which don't really exist. The mean level of the pixels in the overscan region thus gives a measure of the average signal introduced by reading the CCD, i.e. the overscan level. Once this level has been computed, it should be removed from all pixels in the image and hence an image needs to be over scan corrected. We can then trim off the overscan region (keeping only those pixels which correspond to real light-gathering pixels on the CCD). This is called 'trimming' the image. This process of overscan correction and trimming should be done to all images prior to any other pre-processing.

(4) Biasing: It represents the individual pixel-to-pixel variations of the offset level (base level). The bias often has some sort of pattern across the CCD, and does not appear random. The bias is generally fixed, despite variations in the mean offset. That is, apart from noise effects, the difference between the value of a given pixel and the overscan level of the entire image is fixed; regardless of the value of the overscan level. A bias frame is acquired by taking a zero second exposure. In this case the CCD is not exposed to any light, so the measured signal is the bias (+ over scan, which should be removed prior to using the bias frame to de-bias other images). Generally multiple bias frames are acquired and then an average of these frames –"master bias frame" is used to de-bias all the other images. This averaging process ensures that the signal to noise ratio (S/N) of the master bias frame is good enough that the process of de-biasing does not introduce significant extra noise into the corrected images.

(5) Electronic Interference: CCD cameras contain highly incompatible types of electronic circuitry which is very sensitive to any sort of electronic interference. The electronic switching noise from the digital electronics and power noise can easily interfere with the very precise, low-level CCD signals, introducing significant noise into images. It can enter the circuitry either by radiation (EMI) or by being conducted directly through the electrical connections that tie this sensitive circuitry to the rest of the camera electronics. Minimizing the impact of these noise sources in the small, confined space of the CCD camera requires sophisticated mixed-signal design techniques including, careful circuit board layout and isolation, shielding, grounding, signal rise-time control, filtering, and considerate timing. The read noise occurs because the amplifier electronics attached to the CCD are not noiseless. The process of reading the pixels generates a small amount of noise which cannot be removed from a single image, though other noise sources, such as the Poisson noise associated with photons, often dominate.

The optical CCD imager attached to the Himalayan Chandra Telescope (HCT) is based on an E2V 2K X 4K chip with pixel size of 15 micron. The image scale and field covered with this CCD are ideally suited to exploit the telescope under sub-arcsecond seeing conditions.

Table II

CCD	2048 X 4096, 15 micron pixels; thinned, back illuminated, VISAR coated
Image Scale	0.17 arcsec/pixel
FOV	5.9 X 11.8 arcmin
Filters	Bessell UBVRI, I_c, z 372.7(5), 486.1(5), 500.7(5), 656.3(5), 672.4(5), 664.3(10), 680.4(10), 688.4(10), 696.4(10), 704.4(10), 712.4(10), 906.9(10)

Chapter 2.7

WASP-12b

WASP-12b is an extrasolar planet detected using transit method by SuperWASP on the 1st April, 2008. This planet is found to be orbiting the star WASP-12 which is magnitude 11, yellow dwarf star (G- type main sequence star) approximately 871 light years (267 pc) away in the Auriga Constellation. The physical characteristics of WASP-12 and the physical and orbital characteristics of WASP-12b by Maciejewiski G., et al. (2011) and Hebb L., et al. (2009), were found to be as follows:

Table III

Semi-Major Axis	(a)	0.0229 ±0.0008 AU
Orbital Period	(P)	1.09142 days
Mass	(M_P)	1.41 ± 0.10 M_J
Radius	(R_P)	1.79 ± 0.09 R_J
Density	(ρ_P)	0.326 g/cc
Surface Gravity	log(g_P)	2.99 ± 0.03 (cgs)
Inclination	(i)	86 deg
Transit Duration		180.06 mins
Eccentricity	(e)	0.049 ± 0.015
Longitude of Periastron	(ω)	-74^{+13}_{-10} deg
Planet Temperature		2516 ± 36 K
Stellar Radius	(R_*)	1.57 ± 0.07$R_\odot$
Stellar Mass	(M_*)	1.35 ± 0.14$M_\odot$
Stellar Density	(ρ_*)	0.35 ± 0.03$\rho_\odot$
Stellar Effective Temperature		6300^{+200}_{-100} K
Metallicity Fe/H		$0.3^{+0.05}_{-0.15}$
RA		06 30 33
Dec		+29 40 20
Stellar Surface Gravity	log(g_*)	4.17 ± 0.03 (cgs)

The high effective temperature of the central star and short orbital period make WASP-12 b one of the most intensely irradiated extrasolar planets. Due to its close orbit, WASP-12b is one of the lowest density planets. Also as the planet is so close to its parent star (WASP-12) the star's tidal forces are distorting the planet into an egg shape and pulling away its atmosphere at a rate of about 10^{-7} M_J (about 189 quadrillion tonnes) per year. The so-called "tidal heating" and the proximity of the planet to its star combine to bring the surface temperature to more than 2,500 K (2,200 °C). Recent evidence indicates that WASP-12b has a significantly enhanced carbon-to-oxygen ratio than that of the Sun, indicating that it is a carbon-rich gas giant. The C/O ratio compatible with observations is about 1, while the solar value is 0.54. Since the quantity of carbon is more than oxygen, rocks of carbon such as diamond and graphite could be available, hence WASP-12b is also called as the "diamond planet". The Jupiter-mass planet orbits the host star with a period of about 1.09 day causing transits with a depth of 14 milli-mag and duration of 2.7 h. The eccentricity was found to be 0.049 ± 0.015, however further observations showed it to be $0.017_{-0.011}^{+0.015}$. Li et al. (2010) predict that the planet may be losing mass at a rate of $\sim 10^{-7}$ MJ yr^{-1} by Roche lobe overflow. The planetary gas is expected to fall towards the host star through Lagrangian point L1 and form an optically thin accretion disk. The transfer of metals may enhance the apparent stellar metallicity. This effect should be easy to detect because WASP-12 is expected to have a very shallow convective zone. Observations using spectropolarimeter have given some hints of atmospheric pollution in the photosphere of the host star. Observing WASP-12b in near-ultraviolet, Fossati et al. (2010b) detect many metallic atoms and ions in the planetary exosphere, confirmed to exceed the Roche's lobe. WASP-12 b's planetary magnetic field was found to be 2.4×10^{-3} T. No evidences for orbital precision have been found. Li et al. (2010) note that WASP-12b's non-zero eccentricity (if confirmed) could be excited by an additional super-Earth planet embedded in the circumstellar disk. This hypothesis has made WASP-12b an attractive target to search for transit timing variation (TTV) caused by gravitational interactions with an inner perturber. Maciejewiski G., et al. (2011), found that the observed transit timing suggests a short time variation at the level of 3.4σ. Such a TTV signal could be caused by an additional terrestrial-type planet if both planets are close to orbital resonances.

Chapter 3

DEFOCUSED PHOTOMETRY OF WASP-12b TRANSITS

The Principle behind Aperture Photometry:

Instrumental magnitudes are usually measured relative to the sky background in each CCD frame. Prior to measuring the instrumental magnitudes the various instrumental effects should be removed from the CCD frames. Typically bias and flat-field corrections are made and the bad pixels (possibly including whole bad rows and columns) and cosmic-ray events are removed. The principle of aperture photometry is simple. For the star which is to be measured a circular region of the CCD frame (or `aperture') is defined which entirely encloses the image of the star (that is, all the light from the star falls inside the aperture). The flux in all the pixels inside the aperture is added to give the total flux. A similar measurement is made of a region containing no stars to give the flux from the background sky. The two are then subtracted to yield the flux from the star. When doing photometry on crowded star fields, aperture photometry will not yield reliable results. It is better to use a Point Spread Function: a gaussian that can be fitted to all of the stars in the field in order to find their magnitudes.

The Principle behind Defocused Photometry:

The main reason behind defocusing telescopes is that the signal to noise ratio increases with increase in the FWHM. For e.g. consider the FWHM (when the telescope is focused) to be 6 pixels for HCT data, hence the aperture size would be $\pi \times 3^2$ which ≈28.27 pixels. If the average counts/pixel is considered to be 30000 then the total counts for the above aperture size would be about 848100 counts. Now if the expected drop in magnitude (m_{trans} - m) is 0.001 then the counts during the transit would be ≈840292.307 [using $m_{trans} - m = -2.5 \log (f_{trans}/f)$] and hence the drop in counts ($f - f_t$) would be ≈7807. In this case, the signal to noise ratio ($\sqrt{\text{drop in no of counts}}$) would be ≈88.470. However if you consider the FWHM (when telescope is defocused) to be 40 pixels, the aperture size would be ≈1256 pixels and the total counts for this aperture size would be $\approx 3.7699111 \times 10^7$, considering the average counts/pixel to be 30000. Hence the counts during the transit for a drop of 0.001 mag would be 3.7352050×10^7.

Therefore the drop in counts would be ≈34706 and hence the signal to noise ratio would be ≈589.11 which is far greater than that obtained for the FWHM of 6 pixels. This is done by choosing relatively long integration times (several minutes) and dispersing the resulting large numbers of photons over many CCD pixels. This has the huge advantage that flat-fielding errors can be averaged down by orders of magnitude compared to focused observations, and also means that normal changes in atmospheric seeing are irrelevant. Nonlinear pixel responses can be corrected by calibrating the response of the CCD or avoided by sticking to count levels where such effects are low. However the CCD non-linear region is avoided by choosing a suitable exposure time so that maximum counts/pixel is 30000.The longer integration times and large point spread functions (PSFs) mean that the sky background level is much higher than for standard approaches. The PSF considered for the defocused photometry of WASP-12b is 40 pixels (12"), plate scale of HCT is 0.29 and the total no of counts (≈30000 per pixel) are taken as 3.7×10^7.

Brief Summary of the Data Analysis Procedure:

It consists of 3 parts. First to find the magnitudes of the target and reference stars by using the Landolt (standard) star frames and the in-focus object frames. The in-focus frames were taken after the transit period on the same night. Second part is to use PSF fitting photometry on the target star to check for any faint background stars which may contaminate the signal during long exposures. And the third is to do the photometry of defocused frames to obtain the transit light curve.

Step 1: To calculate gain and readnoise from bias and flat filed images.

We consider any two bias frames and any two flats(R filter) and take the difference using imarith which results into a difference bias image and difference flat image. Then select a region free from cosmic rays etc and run imstat on each frame and hence calculate the gain and readnoise using the formulas;

Gain= {(MEAN_F1 + MEAN_F2 - MEAN_B1 - MEAN_B2) \ {(STDDEV_F12^2 - STDDEV_B12^2)}

Readnoise= gain * STDDEV_B12/ $\sqrt[2]{2}$

Gain: The output of a CCD pixel is proportional to the amount of light falling onto it. If we draw a graph with the light intensity on the x-axis and the resulting CCD pixel value on the y-axis we get a straight line starting in the origin for an ideal CCD model. To allow imaging with shorter shutter times or in low light conditions when a longer shutter time is required but not possible the CCD-camera features an amplifier. The amount of amplification is called gain. It is given by electrons per ADU (analog to digital unit).

Readnoise: Noise is unwanted variations in pixel values that make the image a less than exact representation of the original scene. The read noise occurs because the amplifier electronics attached to the CCD are not noiseless.

Gain and readnoise are intrinsic properties of the CCD hence they do not vary.

Step 2: BIASING

Individual pixel to pixel variation of offset (base) level. Bias frames are acquired by taking zero-second exposures.

a. To combine image bias frames to create a master bias.

Create a "zeros.in" file which contains all the bias frames and then run a zerocombine in order to create a "master_bias.fits" frame.

b. Bias, overscan correction and trimming (removal of extra pixels)

For bias and overscan correction on all the frames, create an "obj.in" file which contains all the frames (bias, flats & objects) and run ccdproc. Since the output file is not given all the original files are overwritten (i.e. corrected for bias and overscan). The final images are trimmed to remove the overscan strip.

Step 3: FLAT FIELDING

Variation in the sensitivity of individual pixels because of the optics of the telescope. Mainly due to the variation of Quantum Efficiency (i.e. no the photons striking the CCD to produce signal) across the CCD.

a. To combine flat frames to create a master flat (for U, B, V, R, I filters)

Create different files containing flats in different filters (e.g. "flat_R.in") and run a flatcombine on each so as to get a masterflat in each filter (e.g. "flat_R.out").

b. Flat Correction

Create different files containing only the object frames (in focus & out-of-focus) in each filter (e.g. object_V.in) and run a ccdproc on each so as to get an output file which is corrected for flat-fielding (e.g. object_V.out)

c. Airmass Correction

Create an object_all.out which contains all the object frames (in focus & out-of-focus). Create an airmass.cl script in gedit and then run asthedit so as to correct the airmass for all the object frames.

Airmass: Airmass is the optical path length through Earth's atmosphere for light from a celestial source. As it passes through the atmosphere, light is attenuated by scattering and absorption; the more atmosphere through which it passes, the greater the attenuation (gradual loss in intensity of any kind of flux through a medium). Consequently, celestial bodies at the horizon appear less bright than when at the zenith. The attenuation is known as atmospheric extinction.

Step 4: Aligning and combining image frames (for Landolt-V,R,I filters and In focus Objects-B,V,R,I filters)

The Landolt and the in focus object frames need to be aligned and combined. Hence run an imexamine on all the frames to get the centroids and calculate the X, Y shifts and the average X, Y shifts considering one frame in each filter to be the reference image. The shifts are determined from the centroids of some non-saturated stars in each image. Then create input, output, coordinate and shifts files in each filter (e.g. align77V.in, align77V.out, align_V.coords and shiftsV.in). Next run imalign on the input frames so as to create the output files and then run imcombine on the output frames so as to get a combined and aligned frame. (e.g. LandoltV.fits or ObjectV.fits) {As the CCD is not exactly parallel to the paraboloid mirror hence we do not get doughnut shaped out-of-focus stars and since centroids cannot be accurately found for such out-of-focus images, it is difficult to align the frames}

Step 5: Obtaining Aperture Photometry of Standards and of focused frames (Photometry is carried out on the aligned and combined frames)

a. Setting up parameters - datapars, centerpars, fitskypars, photpars & findpars

b. Finding instrumental magnitude (for Landolt stars and in focus objects)

Set up the parameters and then run daofind so as to get a coordinate file and tvmark to check which stars have been picked up and then phot so as to get a magnitude file. This is to be done on all the aligned and combined frames.

c. Match the landolt frames (to check if the reference stars are present in all the frames) using txdump

d. Defining transformations (using in focus object frames)

Create a file "standstars" which contains the instrumental and standard magnitudes of the standard stars in the frame using the standard star catalogue- http://www.noao.edu/wiyn/queue/images/tableA.html. Create a file "standobs" using "standstars" which contains Field, Filter, airmass (mean), xcentre, ycenter, mag (instrumental), and merr. Create a format file "fstandobs.dat" which corresponds to the format of the standobs file. Run mkconfig on the "standobs" file which will create an "onlandolt.cfg". Make the necessary changes in the transformation equations. Then run fitparams on the "onlandolt.cfg" file to create "onlandolt.ans" and "testlog" files. Create a file "targetrefstars" which includes the Filter, airmass (mean), xcentre, ycenter, mag (instrumental), and merr of the reference stars in the object frames. Create a format file "ftargetrefstars.dat" which corresponds to the format of the targetrefstars file. Run invertfit on the "targetrefstars" file to get a "targetref" file which gives the standard magnitudes.

Hence the standard magnitudes of the target and reference stars are:

Table IV

	V Mag	R Mag	I Mag	V- R mag	V- I mag
WASP-12	11.632	11.545	11.107	0.087	0.525
Ref 1	11.748	11.671	11.247	0.077	0.501
Ref 2	13.115	12.978	12.497	0.137	0.618
Ref 3	12.256	12.116	11.622	0.140	0.634
Ref 4	11.429	11.484	11.235	-0.055	0.194
Ref 5	12.199	11.797	11.128	0.402	1.071

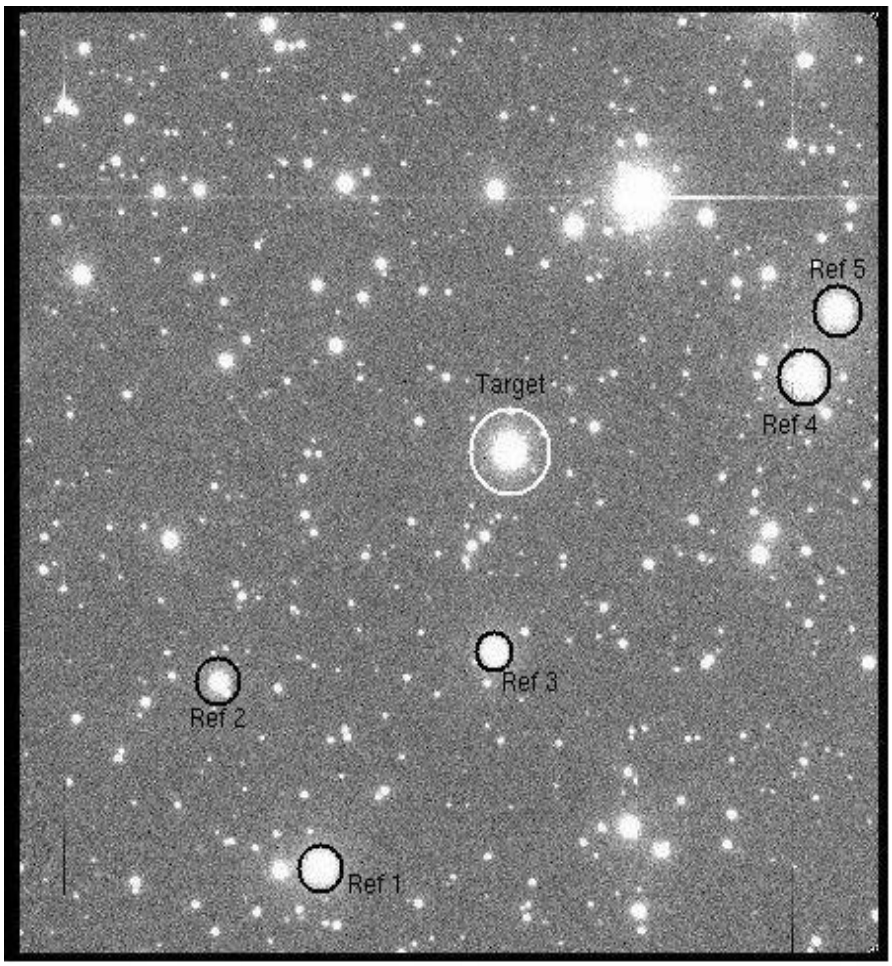

Figure 3.1: Target and Reference Stars

Step 6: Differential Aperture Photometry for out-of-focus stars:

We need to identify target and reference stars and save them in WASP12ref.reg.Find the centroids using imexamine and write the file "WASP12_ref.cor" (where the 1st star is the target star WASP-12).Use the "WASP12_ref.cor" file and a reference frame to calculate the aperture using apcalc. This gives the output file "WASP12_ref.apc".Now to run the vaphot main task, set the parameters photpars, fitskypars, datapars, centerpars and fitpsf. Create "WASP12_list" containing all the out-of-focus object frames. Then run vaphot on this file to get an output file named as "WASP12_(initialFWHM)(max FWHM).vap" which contains (obstime exptime imagename fwhm mag[1]...mag[7] magdiff sky[1] skyavg skystdev airmass). Then run gnuplot in a command window to get the light curve.

Since there are some faint stars close to the target star, we need to do crowded field photometry in order to determine the magnitudes of these faint stars which contribute to the flux of the bright star. It is done to verify if any faint objects are very close to the bright stars.

Step 7: Crowded Field Photometry (in focus object frames)

a. Set the parameters datapars, centerpars, fitskypars, photpars & findpars. Then run daofind on the "ObjectR.fits" frame to get "ObjectR.fits.coo.1" and phot to get "ObjectR.fits.mag.1". We lower the threshold value so as to detect the faint stars.

b. Next Select stars for PSF fitting. Display the image frame "ObjectR.fits" and a tvmark before psf. Then run psf on the "ObjectR.fits" frame to get output files ObjectR.psf.1.fits, ObjectR.pst.1 & ObjectR.psg.1.

PSF: describes the response of an imaging system to a point source or point object. PSF is the impulse response of a focused optical system.

c. Next step is to fit stars with the psf function using nstar and subtract them from your image with substar in order to see how good of a fit you have obtained. Nstar will fit the psf to the stars in the .psg list, and return a .nst file that you can now use with substar to see how well you psf fit worked. Substar will subtract the stars (the reference stars) that have been fitted with the psf function from the original image. This gives an output image - "ObjectR.sub.1.fits". When

substar is done running, display the output file. It is best to open it in a separate frame from the original image, and blink them to see the differences. If there is little to no residuals left over from the subtracted stars, you have got a good psf fit.

d. The next step is to run a simultaneous PSF-fitting on all the stars and produce a subtracted frame with these stars removed. Run allstar to get the output files ObjectR.als.1, ObjectR.arj.1 & ObjectR.sub.2.fits.

e. Next run daofind on the subtracted image frame "ObjectR.sub.2.fits" to get output coordinate file "ObjectR.sub.2.fits.coo.1". Run phot. Note here the input image will be the original frame (to avoid errors due to noise) and the input coordinate file will be the one created from the subtracted frame. Output photometry file ObjectR.fits.mag.2 is created.

f. Now add the stars close to the target and the reference stars to the original magnitude file and create a new magnitude (instrumental) file "ObjectR.fits.mag_combined.1" and run allstar to get the output files ObjectR.als.2, ObjectR.arj.2 & ObjectR.sub.3.fits.

g. To determine aperture correction:

Comparing magnitudes at aperture=15 with magnitudes at aperture=6, consider some isolated stars (they are not as bright as target, but the isolated part is more important) and compare the magnitudes to get the average difference. This is done because when you defined the PSF, the magnitude of the PSF stars were determined using a small aperture (6), however the standard stars were measured through a much larger aperture (15). Hence by doing the aperture correction we measure how much brighter the PSF would have been at the larger aperture (15)

Chapter 4

RESULTS & CONCLUSION

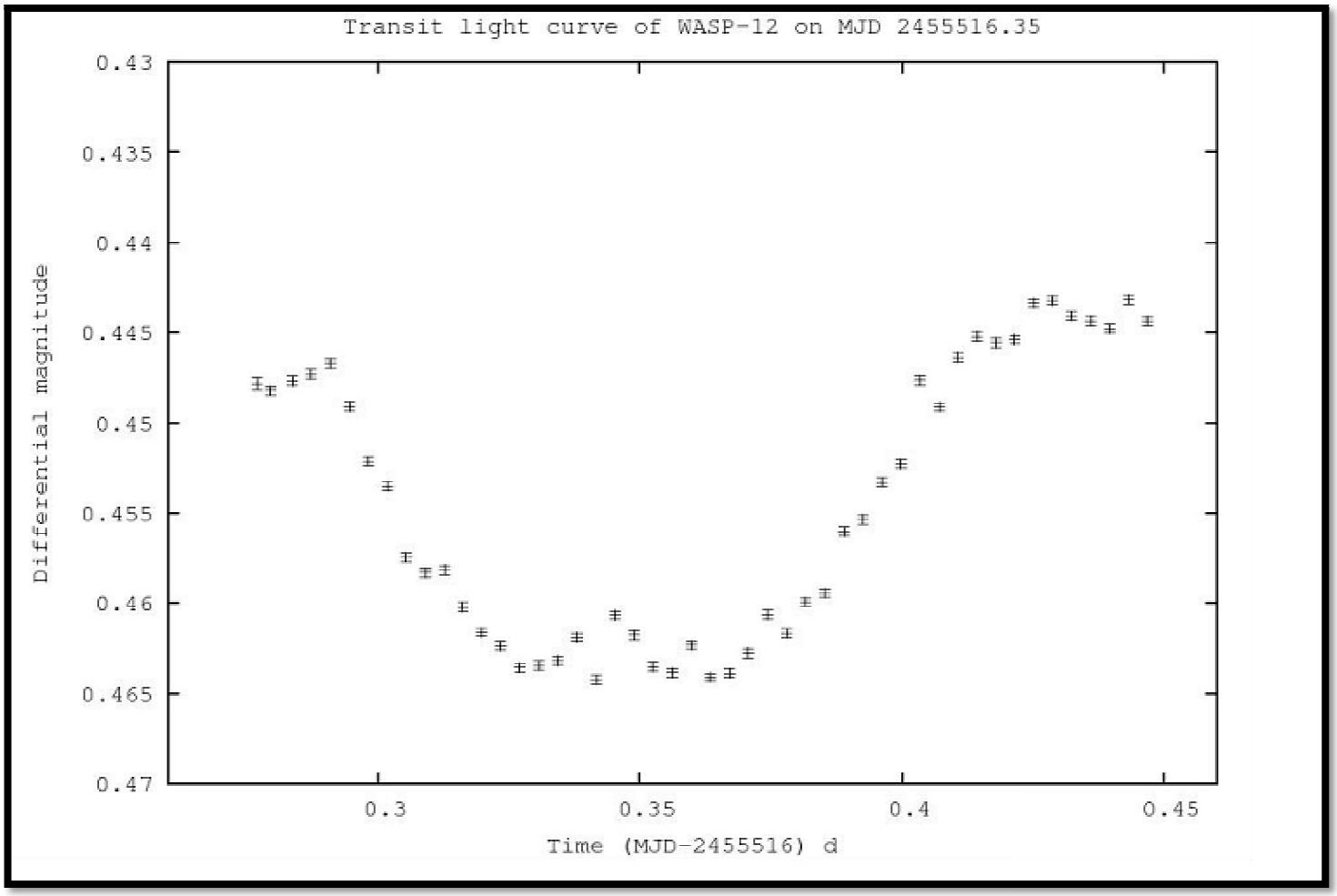

Figure 4.1 : Transit Light Curve of WASP-12b

The above light curve shows the transit depth of around 15 mmag. The photometric error of the individual measurements of the target and reference stars was found to be ranging from 0.3 to 0.4 mmag. The trends in the light curve caused by differential atmospheric extinction can be seen and they need to be corrected. Also another feature seen in the center of the light curve has to be studied. The curvature seen in the ingress and egress of the transit is due to limb darkening effects. The light curve was modelled using the JKTEBOP code. Five parameters describing a shape of a light curve were allowed to float during the fitting procedure. We used fractional radii of the host star and planet, defined as $r^* = R^*/a$ and $r_P = R_P/a$, respectively, where R^* and R_P are the absolute radii of the bodies and a is the orbital semi-major axis. The combinations of these parameters were used, a sum $r^* + r_P$ and ratio $k = r_P / r^*$.

The directly fitted orbital inclination, i, allows calculation of the transit parameter b = acos i / R^*. The initial values of parameters listed above were taken from Maciejewiski G., et al. (2011) and Hebb L., et al. (2009). We considered quadratic LD, for which theoretical LDCs in the Johnson R band were bilinearly interpolated from tables by Van Hamme (1993). We allowed u and v (linear and non-linear coefficients) of the quadratic limb darkening model to vary. The error bars were manually increased to 2 times the calculated value.

The parameters of transit light-curve modelling derived for light curves are:

Table V

Parameters	This work (errors × 2)	Maciejewiski G., et al. (2011) Run #1	Maciejewiski G., et al. (2011) Run #2
$r^* + r_P$ (Sum of radii)	0.39± 0.020	0.374 ± 0.005	$0.382^{+0.016}_{-0.013}$
K (Ratio of radii)	0.105 ± 0.006	$0.11755^{+0.00065}_{-0.00072}$	$0.1188^{+0.022}_{-0.016}$
r^*	0.351199	$0.3342^{+0.0041}_{-0.0042}$	$0.341^{+0.014}_{-0.011}$
r_P	0.037032	$0.03928^{+0.00063}_{-0.00068}$	$0.0406^{+0.0023}_{-0.0018}$
i (deg)	79.53 ± 0.64	$82.2^{+0.8}_{-0.7}$	$81.8^{+1.8}_{-2.4}$
b (R^*)	0.564	$0.391^{+0.041}_{-0.038}$	$0.40^{+0.10}_{-0.13}$
u (quadratic)	1.088 ± 0.182	0.571 ± 0.054	$0.57^{+0.05}_{-0.08}$
T_0 (MJD)	55515.848341130± 0.0002188395	$55230.40146^{+0.00012}_{-0.00010}$	55254.41536 ± 0.00013
rms (mmag)	1.0044319654	0.5840	0.9748
χ^2_{red}	6.1641264827	1.1390	2.8664
v (quadratic)	0.083 ± 0.4	0.2776	0.2776

The Physical properties of the WASP-12 system derived from the light curve:

Table VI

Parameter	This Work	Maciejewiski G., et al. (2011)
R_P (R_J)	1.714	1.9 ± 0.1
ρ (g/cc)	0.3716	0.22 ± 0.04
g_P (m/s^2)	11.4	10.3 ± 0.6
T_{eq} (K)	2639.99	2570^{+100}_{-60}
f (Oblateness)	0.073	0.083

Hence from the above results we conclude that the orbital and radial parameters are confirmed with tighter constraints. Despite the fact that this preliminary analysis of the light curve has been carried out without removing linear and non-linear trends in photometry the physical parameters of the planet and the host star are derived to be very close to the values seen in literature. The results also confirm the distortion of the planet (oblateness) suggesting possible Roche Lobe Overflow. The variations in transit time are observed. However further studies are required.

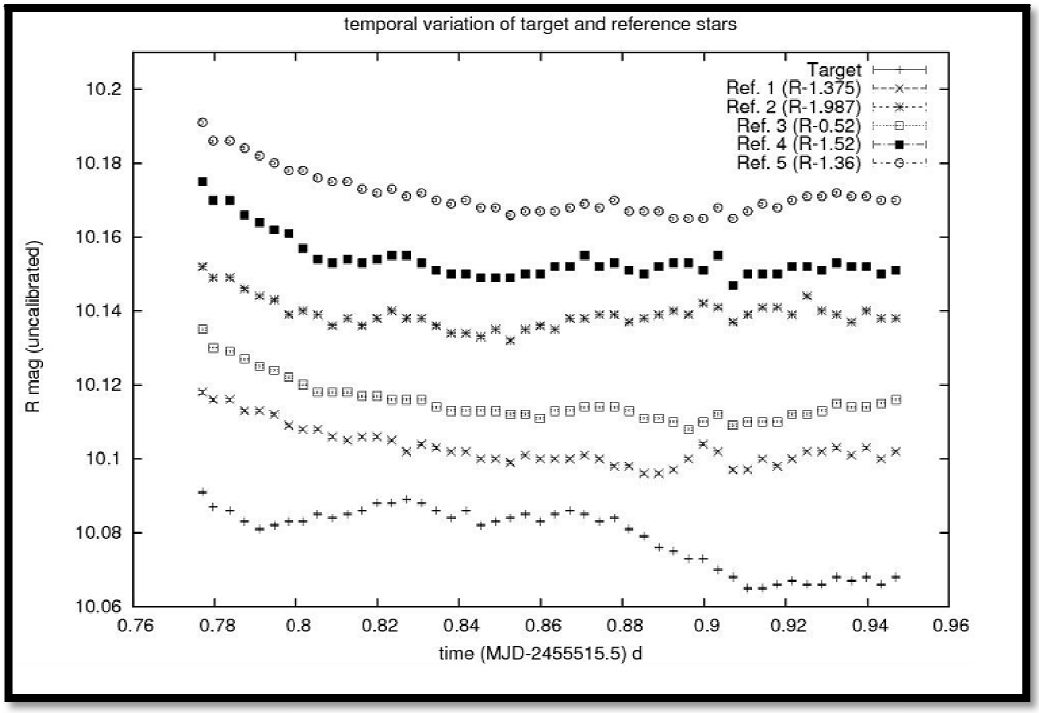

The above plot shows the temporal variations of the target and reference stars. The variation seen in all stars around 0.9 + 2455515.5 MJD is most likely an artifact of photometry. It is seen that the stars also have an intrinsic variation of about 5 mmag. The reference stars 2 and 4 also show a feature at around 0.83 + 2455515.5 MJD. The error bars are typically of the order of 0.3 to 0.4 mmag. These features are yet to be studied. A general trend of the star brightening towards the end of the night is also seen. Earlier studies of photometric variability in stars with HCT have shown that PSF changes throughout the night.The variation of FWHM with time as seen in the study of photometric variability of stars in NGC 5024 is shown in the figure below reproduced from Safonova, M., and Stalin, C.S., ``Variables in Globular Cluster NGC 5024", 2011, \\AJ, submitted.

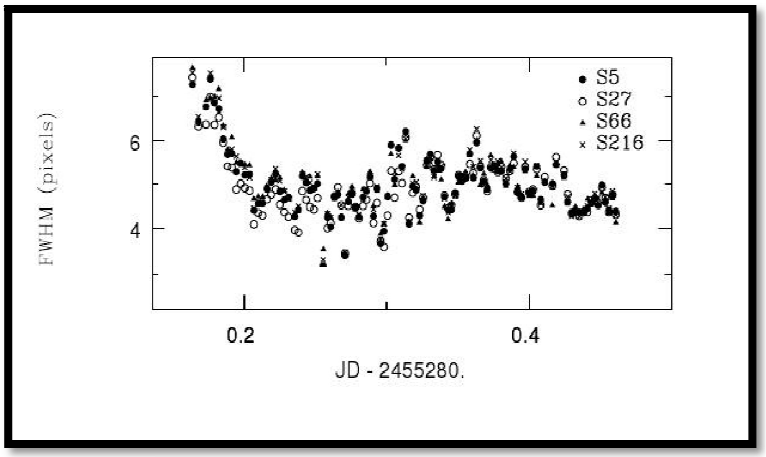

Chapter 5

COMPARING EXTRASOLAR PLANETS WITH THE SOLAR SYSTEM PLANETS

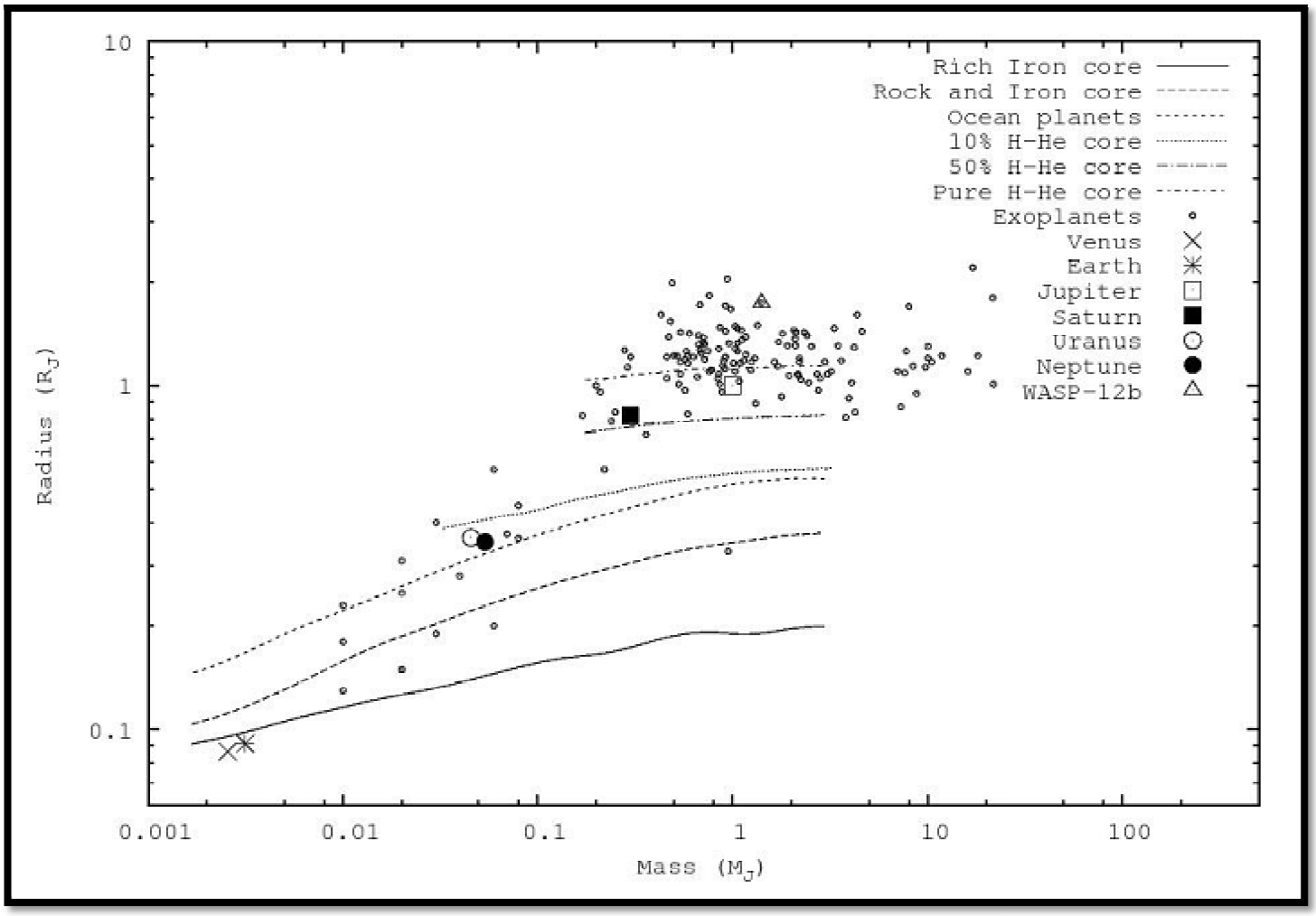

Figure 5.1 : Graph of Radius Vs Mass for known exoplanets

The above plot is a comparison between the extrasolar planets with known radii and masses with the solar system planets. It is observed that for the extrasolar planets with mass greater than 1 M_J, the mass becomes independent of the radius. Brown dwarfs are sub-stellar objects which are too low in mass to burn H via fusion reactions in their cores. In case of brown dwarfs their volume is governed by Columb pressure and/or electron degeneracy pressure. In the case of the latter the mass of brown dwarf becomes independent of their radius. Hence these extrasolar planets for which the mass becomes independent of the radius may possibly be brown-dwarfs.

It is also observed in the above plot that most of the extrasolar planets lie above the pure hydrogen- helium core. WASP-12b, a carbon rich gas giant (shown by Δ), is found above the pure hydrogen- helium core.

Interior Structures of the Solar System Planets:

Mercury: Mercury has a mean density of 5.44 g/cc. The outer layer is composed of magnesium-silicates with a density of 3.3 g/cc and the molten core is composed of pure γ-iron (Fe or Fe-S) with a density of 8.95 g/cc. Mercury has an intrinsic magnetic field.

Venus: Venus has a mean density of 5.25 g/cc. As its mass is 0.81 M_{earth} it is considered to have an interior similar to that of the Earth. Venus has no detectable intrinsic magnetic moment. The absence of sulphur in the core causes its core to solidify at the same temperature for which Earth's core is partly molten due to presence of sulphur. However sulphur is observed in Venus's atmosphere. The bulk iron fraction in Venus lies between the terrestrial values of ~0.4 to the solar value of ~0.3.

Earth: The interior of the Earth has been divided into five zones namely, the crust, the upper mantle, the lower mantle, the outer core and the inner core. The crust contains lower density silicates containing magnesium, aluminum, calcium, sodium and potassium. Oceanic Crust is basalt with high magnesium content. The upper mantle consists mainly of silicates of iron and magnesium and the lower mantle consists of olivine and pyroxene. Earth has an iron rich core which is very close to 1/3 of the total mass of Earth. The core also contains small amounts of lighter elements in addition to the iron content. Earth has a mean density of 5.515 g/cc.

Mars: The composition of Mars is similar to that of the Earth. Mars contains a core composed of iron, nickel, cobalt and sulphur and the mantle is composed of FeO and silicates. The crust is mainly basalt and is covered with finely grained iron oxide. Mars has a mean density of 3.934 g/cc.

Jupiter: Jupiter has an iron central core surrounded by silicates. The core is surrounded by higher molecular materials containing metallic hydrogen, helium and carbon. The outermost layer consists of molecular hydrogen. Its mean density is 1.326 g/cc.

Saturn: It is the lowest mean density ~0.687 g/cc planet containing a silica metal core surrounded by metallic hydrogen followed by liquid hydrogen, helium layer.

Uranus: Uranus with a mean density of 1.27 g/cc is composed of a silicate/iron-nickel core followed by an icy mantle, generally methane and outer gaseous hydrogen/helium layer.

Neptune: Neptune's internal structure resembles Uranus and has a mean density of 1.638 g/cc. The mantle is rich in water, ammonia and methane and the core is composed of iron, nickel and silicates.

Pluto (dwarf Planet): Pluto has a mean density of 2.03 g/cc and consists of a dense core surrounded by a mantle of ice.

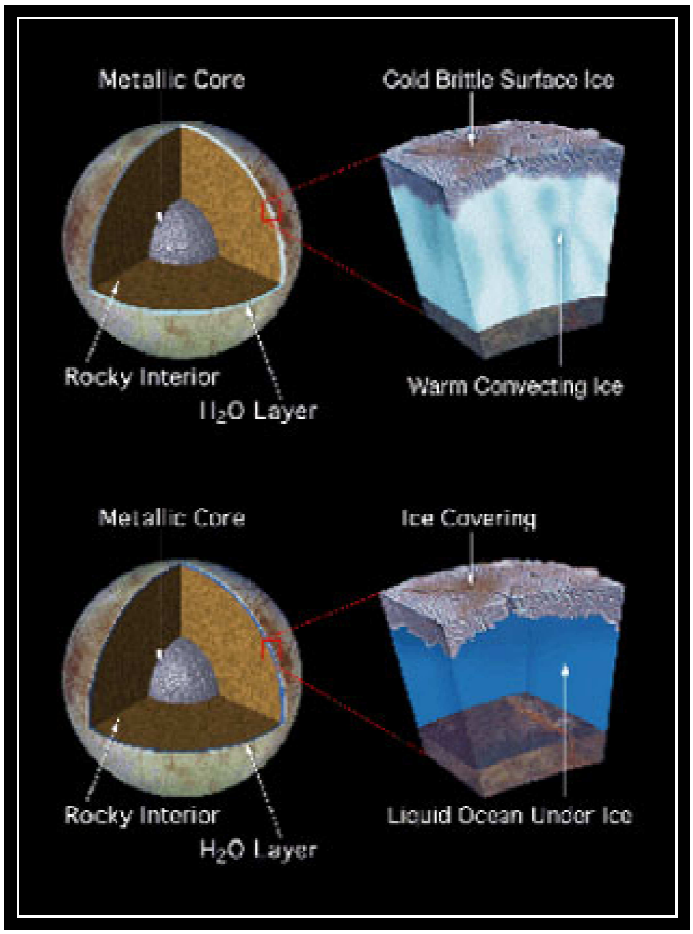

Figure 5.2 : Interior Structure of Planets

REFERENCES

- Detection Methods and Properties of Known Exoplanets, Patrick G. J. Irwin, in "Exoplanets – Detection, Formation, Properties, Habitability", Edt. John. W. Mason, (2008), Springer, Praxis Publishing Ltd.
- Detection of Extrasolar Planets by Gravitational Microlensing, David P. Bennett, in "Exoplanets – Detection, Formation, Properties, Habitability "Edt John. W. Mason, (2008), Springer, Praxis Publishing Ltd.
- The New Worlds – Extrasolar Planets, Fabienne Casoli and Therese Encrenaz, (2005), Springer, Praxis Publishing Ltd.
- Extrasolar Planets: Formation, Detection and Dynamics, Etd. Rudolf Dvorak, (2008), Wiley-VCH.
- Photometry and Exoplanets, in Stars, Exoplanets and the Search for life, Ignacio Ferreras (UCL), (2011), L11, PHAS 1512.
- The Transits of Extrasolar Planets with Moon, David Mathew Kipping (UCL), (2011), (Project Report).
- Analysis of Exoplanetary Transit Light Curves, Joshua Adam Carter (MIT), (2009), (Project Report).
- Planets: Their Origin, Interior and Atmosphere, D. Gautier, W.B. Hubbard and H. Reeves, (1984), Geneva Observatory.
- Planetary Science- The Science of Planets around stars, George H A Cole, Michael M Woolfson, (2002), IOP Publishing Ltd.
- Extrasolar Planets, P. Cassen, T. Guillot, A. Quirrenbach, (2006), Springer.
- Interiors of the Planets, A.H. Cook, (1980), Cambridge University Press.
- Extrasolar Planets, Dimitar D Sasselov, (2008), Nature, Vol 451, Pages 29, 30, 31.
- Exoplanet Transit Spectroscopy and Photometry, S. Seager, (2008), Space Sci Rev., 135:345-354, Springer.
- Transits and Occultations, Joshua N. Winn (Massachusetts Institute of Technology), (2011), Project Report.

- High Precision Photometry of WASP-12b transits, G. Maciejewski, R. Errmann, St. Raetz, M.Seeliger, I. Spaleniak and R. Neuhäuser, (2011), A&A, **528**, A65
- High-precision photometry by telescope defocusing. I. The transiting planetary system WASP-5, Southworth J., et al., (2009), MNRAS, **396**, 1023.
- Transit timing variation in exoplanet WASP-3b, Maciejewiski G., et al., (2010), MNRAS, **407**, 2625.
- WASP-12b: the hottest transiting extrasolar planet yet discovered, Hebb L., et al., (2009), The Astrophysical Journal, 693:1920-1028.
- WASP-12b as a prolate, inflated and disrupting planet from tidal dissipation, Li L., Miller N., Lin D. N.C., & Fortney J. J. , (2010) , Nature, 463, 1054.
- SuperWASP- http://www.superwasp.org/
- Exoplanet Transit Database - http://var2.astro.cz/ETD/
- The Extrasolar Planet Encyclopedia - http://exoplanet.eu/
- Exoplanet Transit Database | Exoplanet Data Explorer - http://exoplanets.org/
- Visual Exoplanet Catalogue- http://exoplanet.hanno-rein.de/

LIST OF FIGURES AND TABLES